Neurobiology of Aging 81 (2019) 88–101

Contents lists available at ScienceDirect

Neurobiology of Aging

journal homepage: www.elsevier.com/locate/neuaging

Short erythropoietin-derived peptide enhances memory, improves long-term potentiation, and counteracts amyloid beta–induced pathology

Oksana Dmytriyeva [a,b,1], Amor Belmeguenai [c,d,1], Laurent Bezin [c,d], Katia Soud [a], David Paul Drucker Woldbye [a], Casper René Gøtzsche [a], Stanislava Pankratova [a,b,*]

[a] Laboratory of Neural Plasticity, Department of Neuroscience, University of Copenhagen, Copenhagen, Denmark
[b] Research Laboratory for Stereology and Neuroscience, Bispebjerg-Frederiksberg Hospital, Copenhagen University Hospital, Copenhagen, Denmark
[c] Lyon Neuroscience Research Center, TIGER Team, Bron, France
[d] Epilepsy Institute IDÉE, Bron, France

ARTICLE INFO

Article history:
Received 25 April 2018
Received in revised form 27 March 2019
Accepted 6 May 2019
Available online 13 May 2019

Keywords:
Erythropoietin-derived peptide
Neuroprotection
Memory
Beta amyloid peptide$_{25-35}$
Hippocampus
Neurite outgrowth

ABSTRACT

Neurodegenerative disorders such as Alzheimer's disease (AD) are characterized by the irreversible neuronal loss and memory impairment, and current treatments are merely symptomatic. Erythropoietin (EPO) has been shown to possess neurotrophic, neuroprotective, anti-inflammatory, and memory-enhancing effects, which could be therapeutically beneficial in the different aspects of AD. However, the hematopoietic effect of EPO has hampered its potential as a neuroprotective and procognitive agent. In this study, we characterized a novel small peptide, NL100, derived from a conserved C-helix region of EPO. NL100 was shown to bind to the EPO receptor, induce neuritogenesis, and protect hippocampal neurons from oxidative- and Aβ_{25-35}-induced neurodegeneration in vitro. Importantly, long-term NL100 treatment did not induce hematopoiesis, overcoming this challenge associated with EPO. Memory-enhancing effects were demonstrated after NL100 treatment in social recognition test for short-term memory, in both healthy rats and rats challenged centrally with Aβ_{25-35} peptide, and in the Morris water maze test for spatial memory. Moreover, NL100 was shown to reverse Aβ_{25-35}-induced hippocampal degeneration and gliosis as well as pilocarpine-induced suppression of long-term potentiation in rats. In conclusion, NL100 is a novel EPO-derived nonhematopoietic peptide with neuroprotective and memory-enhancing effects and could therefore be a potential candidate for the development of new treatments for neurodegenerative disorders and dementia.

1. Introduction

Neurodegenerative diseases such as Alzheimer's disease are characterized by the progressive and irreversible loss of neuronal cells and decline in cognitive functions (Metcalfe et al., 2017). Current treatments are not disease modifying but merely alleviate symptoms, and new therapies possessing neuroprotective and memory-enhancing effects are highly warranted. Erythropoietin (EPO) is a 30.4 kDa pleiotropic growth factor, critically involved in red blood cell production. Apart from this, it plays important roles in the central nervous system (CNS), during development, and is a well-established neurotrophic and neuroprotective factor, helping the adult brain to counteract various injuries (Brines and Cerami, 2005; Maiese et al., 2012; Sargin et al., 2010; Siren et al., 2009; Yu et al., 2002). Systemic EPO is produced by interstitial fibroblasts in the kidneys and has been shown to cross the blood-brain barrier (BBB) to enter the CNS in rodents and humans (Brines et al., 2000; Statler et al., 2007). In addition, EPO and its receptor (EPOR) are expressed locally in the brain by neurons, astrocytes, oligodendrocytes, and cerebral endothelial cells (Brines et al., 2000; Lee et al., 2012; Ott et al., 2015; Sanchez et al., 2009). The canonical signaling of EPO is involved in regulating neuronal plasticity, neuroprotective, anti-apoptotic, and anti-inflammatory activities (Maiese et al., 2012; Sargin et al., 2010; Siren et al., 2009; Yu et al., 2002). Notably, systemically injected EPO improves neurological functions and reduces brain damage after traumatic brain and spinal cord injuries (Brines et al., 2000; Celik et al., 2002; Gantner et al., 2017; Li et al., 2016b; Ning et al., 2011), cerebral ischemia (Sakanaka et al., 1998; Siren et al., 2001), experimental autoimmune

* Corresponding author at: Laboratory of Neural Plasticity, Department of Neuroscience, University of Copenhagen, Blegdamsvej 3, Copenhagen 2100, Denmark. Tel.: +4525624325; fax: +4535453264.
E-mail address: stasya@sund.ku.dk (S. Pankratova).
[1] These authors contributed equally to this work.

0197-4580/$ – see front matter © 2019 Elsevier Inc. All rights reserved.
https://doi.org/10.1016/j.neurobiolaging.2019.05.003

encephalomyelitis (Li et al., 2004), and status epilepticus (SE) (Chu et al., 2008).

At the behavioral level, EPO treatment has been shown to improve cognitive functions, in both healthy volunteers (Miskowiak et al., 2008b) and patients with chronic kidney disease (Grimm et al., 1990; Kambova, 1998; Pickett et al., 1999), neuropsychiatric disorders (Ehrenreich et al., 2007; Miskowiak et al., 2014), and type-1 diabetes (Kristensen et al., 2013), instigating further research to elucidate the mechanisms of the cognitive-enhancing effect of EPO. In corroboration, EPO has been shown to improve long-term potentiation (LTP) and memory in healthy mice (Adamcio et al., 2008; El-Kordi et al., 2009) and to reduce cognitive and behavioral deficits induced by ischemia and reperfusion injuries, diabetes, traumatic brain injuries, and mechanical hippocampal trauma (Lu et al., 2005; Mogensen et al., 2008; Xiong et al., 2009). Transgenic mice expressing constitutively active neuronal EPOR showed improved cognitive and learning performance (Sargin et al., 2011). The underlying mechanisms of EPO-induced improvement of cognitive functions are likely multifaceted and may include alterations in short- and long-term neuroplasticity, affecting hippocampal synaptic transmission and connectivity (Adamcio et al., 2008; Almaguer-Melian et al., 2016; Byts and Siren, 2009). In addition, the antioxidative effects (Barichello et al., 2014; Bond and Rex, 2014) of EPO together with its ability to attenuate secondary injury (Brines and Cerami, 2005) and ameliorate endothelial degeneration (Lee et al., 2012) could add further explanation to the beneficial effects of this cytokine in degeneration- and pathology-induced cognitive dysfunctions (Miskowiak et al., 2012). Analysis of various preclinical epileptic seizure models indicates that neuroprotective and anti-apoptotic effects of systemically administered EPO (Nadam et al., 2007; Sozmen et al., 2012) are accompanied by decreases in BBB permeability (Uzum et al., 2006) and anti-inflammatory effects (Bahcekapili et al., 2014). The latter is of importance because proinflammatory cytokines downregulate the expression of endogenous EPO (Brines and Cerami, 2005), thus making exogenously applied recombinant EPO or its mimetics therapeutically valuable. Consistently, EPO prevents neuronal and microglia toxicity, induced by beta-amyloid (Aβ) in vitro (Chong et al., 2005; Ma et al., 2009; Shang et al., 2012; Sun et al., 2008). In mouse models of Alzheimer's disease (AD), multiple i.p. dosing with EPO or intranasal delivery of EPO, formulated in form of low-sialylated protein, improved memory, promoted endothelial regeneration, and decreased the number of amyloid plaques in hippocampus (Lee et al., 2012; Maurice et al., 2013; Rodriguez Cruz et al., 2017), probably via upregulation of the Aβ-degrading enzyme, neprilysin (Danielyan et al., 2009). Thus, the neuroprotective and memory-enhancing effects of EPO make it an intriguing candidate for the development of new treatments targeting AD and other neurodegenerative diseases, where neuronal cell death and impaired cognition are centrally involved.

The treatment of neurological disorders requires continuously and longitudinal systemic administrations of drugs formulated as small molecules, which easily cross the BBB and do not possess unfavorable side effect profiles. In light of this, the potential of EPO as a neuroprotective agent is hampered by its canonical hematopoietic effects and other side effects (e.g., hypertension, thrombosis, and tumor progression) (Brines and Cerami, 2005; Maiese et al., 2012; Miskowiak et al., 2012, 2014), as well as its relatively large size of 30.4 kDa. One of the ways to circumvent these limitations is to use nonhematopoietic EPO modifications (i.e., carbamylated EPO, asialoEPO (Erbayraktar et al., 2003; Leist et al., 2004)), EPO mutants (Dhanushkodi et al., 2013; Zhang et al., 2019), or small peptide mimetics (pHBSP/ARA90; Epotris, Epobis; JM4) (Brines et al., 2008; Dmytriyeva et al., 2016; Pankratova et al., 2010, 2012; Wang et al., 2016). Importantly, the aforementioned EPO formulations and peptide mimetics can readily cross the BBB and have shown neurotrophic and neuroprotective functions, confirmed in various in vitro and preclinical models, further supporting the observation that the neuroprotective potential of EPO is unrelated to its hematopoietic effect (Siren et al., 2009). While the neuroprotective effects of the EPO mimetics are well studied in various preclinical models, the effects on cognitive functions are only evaluated for few nonhematopoietic peptides, ARA290 and Epobis, which have been demonstrated to increase the attention toward images with positive emotion contents in healthy volunteers (Cerit et al., 2015) and to improve working memory in rats (Dmytriyeva et al., 2016), respectively. In addition, pHBSP peptide, mimicking the surface of EPO helix B, improves memory after mild traumatic brain injury in rats (Robertson et al., 2013).

We have previously developed a nonerythropoietic neurotrophic peptide, Epotris, designed after the binding site of EPO to its canonical EPOR (Dmytriyeva et al., 2016; Pankratova et al., 2010). We demonstrated that the Epotris motif, corresponding to C-helix of EPO, sequence-specifically binds to and activates EPOR and promotes neuritogenesis and neuronal survival both in vitro and in vivo. Furthermore, this 20-mer tetrameric peptide crosses the BBB and has anti-epileptic activities in vivo, by decreasing seizure severity and mortality in the kainic acid–induced seizure model (Pankratova et al., 2010), as well as attenuating pilocarpine-induced status epilepticus (Zellinger et al., 2011). The sequential N- and C-terminal truncations of the Epotris peptide followed by functional in vitro test delineated a minimal functional 12-mer motif with neurotrophic activity similar to the 20-mer Epotris peptide (Pankratova et al., 2010). To improve the feasibility of developing drugs for potential clinical application, it is important to scrutinize the size of CNS-targeted molecule, without compromising its therapeutic effects. Therefore, in this study, we formulated the minimal functional 12-mer EPO-mimetic peptide in the dimeric form, termed NL100, and evaluated its hematopoietic, neurotrophic, and neuroprotective effects, and explored its procognitive potential under physiological conditions, in the ex vivo response to pilocarpine-induced SE, and in an in vivo model of $A\beta_{25-35}$ toxicity.

2. Materials and methods

2.1. Peptides

The NL100 peptide, corresponding to the human EPO sequence ($_{127}$SGLRSLTTLLRA$_{138}$, Uniprot P01588), was synthesized as a dimer, composed of 2 peptide chains coupled to a lysine backbone, using the solid-phase Fmoc protection strategy (Schafer-N, Copenhagen, Denmark). The molecular weight of the NL100 peptide was 2843.4 g/mol. The NL100 peptide possessed >80% purity, as determined by high-performance liquid chromatography.

The $A\beta_{25-35}$ peptide (Bachem, H-1192; Bubendorf, Switzerland) was dissolved in sterile water (3 mg/mL) and stored at −20 °C. Before the application, the amyloid peptide was allowed to aggregate for 4 days at 37 °C (Delobette et al., 1997; Fedotova et al., 2016). To monitor the fibrillization of $A\beta_{25-35}$ peptide over time, the peptide samples were diluted in Tris buffer (pH 7.4) to the final concentration 100 μM and incubated with thioflavin T (ThT, 0.5 mM; Sigma-Aldrich, Brøndby, Denmark) at 37 °C for 4 days. ThT is known to increase fluorescence, upon binding to amyloid fibrils. The samples of ThT/Tris buffer without $A\beta_{25-35}$ peptide were used as a negative control. Fluorescence of ThT was measured by excitation set to 450 nm and emission set to 485 nm.

2.2. Surface plasmon resonance

Binding analysis was performed with surface plasmon resonance (SPR) spectroscopy, a label-free optical technique, which allows monitoring highly specific bimolecular interaction of an analyte in the mobile phase with an immobilized at the sensor surface protein in real time. Analysis was performed with a BIAcore 2000 instrument (Pharmacia Biosensor AB, Uppsala, Sweden) and carried out on HBS-EP as running buffer (10 mM Hepes, 150 mM NaCl, 3 nM EDTA, 0.005% Tween-20, pH 7.4). In 3 independent experiments, 1100-1400 RU of human EPOR-Fc (R&D Systems, Minneapolis, MN) was immobilized covalently at a flow rate of 5 μL/min by an amine-coupling procedure, according to the manufacturer's instructions. Briefly, the CM4 sensor chip was activated with 25 μL of activation solution, followed by injection of either EPOR-Fc or control IgG (R&D Systems), diluted in 10 mM sodium acetate (pH 5). Then, the flow cell was deactivated with 25 μL of ethanolamine-HCl (pH 8.5) and washed with running buffer.

To verify the functionality of immobilized EPOR, the recombinant human EPO (rhEPO; R&D Systems) was injected over the chip at a flow rate of 50 μL/min, followed by regeneration with 10 mM Glycine-HCl (pH 2). To estimate the binding kinetics of the NL100 peptide to EPOR, peptide samples in 6 serial dilutions were injected at a flow rate of 30 μL/min and tested in duplicates at 25 °C. Curves were double-referenced by sequentially subtracting first the corresponding curves for binding to a blank well, followed by subtraction of a control curve, obtained by injection of the running buffer alone. Obtained curves were analyzed using the BIAevaluation software package, version 4.1 (Pharmacia Biosensor AB). Curves were fitted using a 1:1 interaction model, and the equilibrium dissociation constant (K_D) was calculated as k_d/k_a, where k_a and k_d are the association and dissociation rate constants, respectively.

2.3. Assessment of neurite outgrowth effects

Embryonic day 19 rat hippocampal neurons were isolated from Wistar rats (Charles River, Sulzfeld, Germany), as previously described (Pankratova et al., 2012), plated at a density of 1×10^4 cells/cm^2 in eight-well LabTek Permanox chamber slides (NUNC, Roskilde, Denmark) in neurobasal medium with supplements (2% B27, 2 mM GlutaMAX, 20 mM HEPES, 100 U/mL penicillin, and 100 μg/mL streptomycin), and stimulated with rising concentrations of the NL100 peptide for 24 hours. Neurons were then fixated with 4% v/v formaldehyde in phosphate-buffered saline (PBS) and immunostained with polyclonal rabbit anti-rat growth-associated protein−43 antibodies (1:1000; Chemicon, Temecula, CA), followed by incubation with Alexa Fluor 488 conjugated secondary antibodies (1:1000; Invitrogen, Copenhagen, Denmark).

2.4. Analysis of neuronal survival

Hippocampal neurons were plated at a density of 5×10^4 cells/cm^2 in poly-L-lysine-coated eight-well LabTek Permanox chamber slides, as previously described (Pankratova et al., 2012). After 7 days in culture, neurons were treated with the serially diluted NL100 peptide, followed 1 hour later by the addition of 80 μM freshly prepared H_2O_2 (Sigma-Aldrich) or 25 μM preaggregated $A\beta_{25\text{-}35}$. Cells were cultured for additional 24 hours (oxidative stress) or 48 hours ($A\beta_{25\text{-}35}$-toxicity), before being fixated as described previously, and stained with 5 μg/mL Hoechst 33258 (Invitrogen, Taastrup, Denmark). At least 1000 cells/condition were recorded systematically by computer-assisted fluorescent microscopy, and cell viability was estimated, based on nuclei morphology, as previously described (Pankratova et al., 2012). The results are expressed as the mean of the live cell ratio: N live cells/(N live cells + N dead cells) ± SEM.

2.5. Animal experiments

All experiments with animals were approved by the Danish Animal Experiments Inspectorate or performed in accordance with the guidelines of the Animal Care and Use Committee of the University Claude Bernard Lyon 1. Female BALB/c mice were obtained from Taconic (Ejby, Denmark). Male Wistar rats were obtained either from Taconic (Lille Skensved, Denmark) or Charles River (Sulzfeld, Germany), whereas Sprague-Dawley male rats were from Harlan (Horst, The Netherlands). Animals were adapted to the laboratory housing conditions for 7 to 10 days before testing.

2.6. Hematopoietic activity and pharmacokinetics of NL100

Male Wistar rats (220–250 g) were habituated and randomly assigned to 4 treatment groups (n = 6) treated s.c. with NL100 in doses of either 5 or 15 mg/kg, EPO (10 μg/mg; Calbiochem), or vehicle (saline) twice per week for 5 weeks. To perform the independent evaluation in mice, female BALB/c mice, weighing 24–25 g, were randomly assigned to received subcutaneous (s.c.) injections of NL100 (14 mg/kg), EPO (5 μg/kg), or vehicle (PBS) twice per week for 5 weeks. Blood samples were collected from the retro-orbital plexus (mice) or tail vein (rats) with end-to-end capillary tubes (Virtex, Copenhagen, Denmark) once per week in EDTA-coated tubes (BD, Plymouth, UK). The hemoglobin (Hb) level was determined, using an automated analyzer (KX-21N, Sysmex, Mundelein, IL) with adapted dilutions. Hematocrit values were measured by microcapillary centrifugation (HC-240, Boeco, Germany). The experimenter conducting hematopoietic study and data analysis was blinded to treatment conditions in experiment with mice only. For the pharmacokinetics experiment, biotinylated NL100 (bNL100; 5 mg/kg) was administered s.c. to male Wistar rats (360–430 g), and blood sampling was performed at different time points under fentanyl (0.002%, w/v), droperidol (0.14%, w/v), and midazolam (0.014%, w/v) anesthesia. Cerebrospinal fluid (CSF) was collected from cisterna magna 1 hour after single s.c. administration of bNL100 under deep anesthesia as described previously (Rudenko et al., 2010). Detection of bNL100 peptide in plasma and CSF was performed by competitive ELISA essentially as described previously (Dmytriyeva et al., 2016; Pankratova et al., 2010).

2.7. Social recognition test

The test was performed on male Wistar rats in 2 independent setups, using either healthy rats (n = 12 per group) or $A\beta_{25\text{-}35}$-challenged rats (sham n = 12, $A\beta_{25\text{-}35}$ n = 11, $A\beta_{25\text{-}35}$+NL100 n = 11). Within each setup, rats were randomly assigned to groups and treated s.c. (1 mL/kg) with either NL100 (5 mg/kg) or vehicle, 24 hours and 1 hour before the test, which was performed as previously described (Klementiev et al., 2007; Secher et al., 2006). Briefly, on the day of the experiment, adult animals were individually housed in transparent cages (30×25×19 cm) 1 hour before testing. The test consisted of an initial trial, followed by 2 hours (for healthy rats) or 30 minutes (for $A\beta_{25\text{-}35}$-challenged rats) intertrial interval and a test trial. In the initial trial, the adult test rat was introduced to a 3-week-old juvenile male rat for 4 minutes, and the time spent on investigation behavior (e.g., licking, sniffing, chewing, and close following) by the test rat toward the juvenile was scored. To verify that any observed effects were plausibly related to modulatory effects on social memory, a control test was performed with an additional group of rats under the same experimental

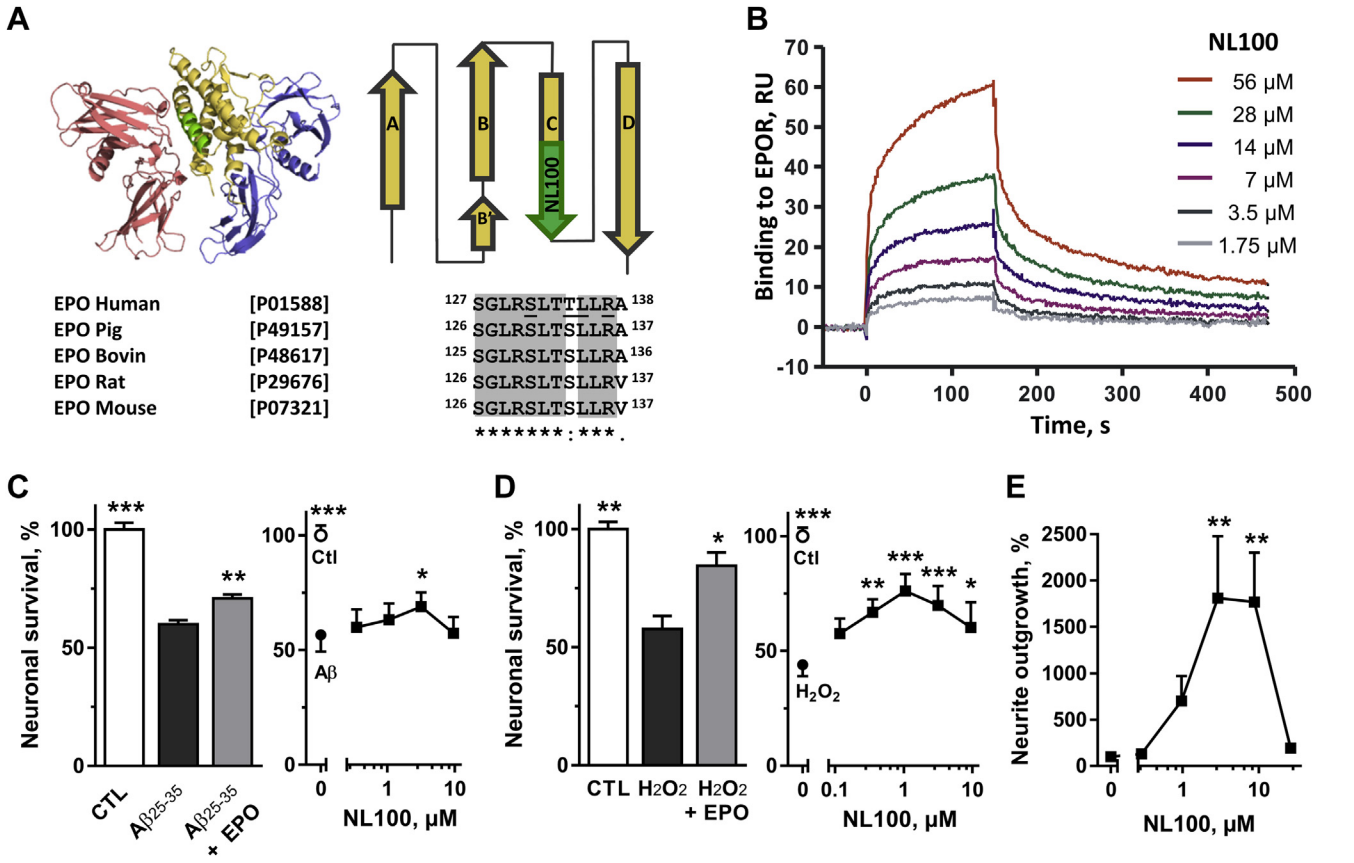

Fig. 1. The NL100 peptide binds to EPOR and promotes the neurotrophic and prosurvival effects in vitro. (A) Ribbon diagram of the EPO:EPOR$_2$ complex (top left; Protein Data Bank [PDB] accession number 1EER) and schematic diagram of the 4 α-helices of EPO molecule (top right; helices A, B, C, and D), showing the location of the NL100 motif in helix C (highlighted in green). The alignment of the NL100 motif across mammalian species shows the conserved amino acids (depicted with gray boxes). The side chains known to be involved in the EPO:EPOR$_2$ intermolecular interaction are underlined. (B) Surface plasmon resonance analysis shows the binding of immobilized EPOR to the NL100 peptide. Serially diluted peptide samples were injected in duplicates and 3 independent experiments were performed. The K_D value of NL100:EPOR binding is 4.2 ± 0.8 μM. Effect on the survival of hippocampal neurons, which were challenged with A$\beta_{25\text{-}35}$ (C) or H_2O_2 (D) alone or supplemented with either 14 nM EPO (C, D, left) or serially diluted NL100 peptide (C, D right). Results from 4 to 6 independent experiments are shown as mean ± SEM compared to untreated controls, set as 100%. (E) Quantification of neurite outgrowth from the primary hippocampal neurons grown for 24 hours in the presence of serially diluted NL100 peptide. $^{**}p < 0.01$; compared to unstimulated control, set as 100%. $^{*}p < 0.05$; $^{**}p < 0.01$; $^{***}p < 0.001$; one-way ANOVA, followed by Dunnett's multiple comparisons tests. Abbreviations: Aβ, amyloid beta; CTL, control; EPO, erythropoietin; EPOR, erythropoietin receptor; RU, resonance units. (For interpretation of the references to color in this figure legend, the reader is referred to the Web version of this article.)

settings as those described previously, with the only exception that an unfamiliar juvenile rat was introduced in the test trial. In the set up with healthy animals, the same test was repeated after 72 hours, to investigate long-term effects of NL100 treatment.

The social recognition ratio (SRR) was calculated as T2/(T1+T2), where T1 and T2 are the time spent investigating the juvenile by the adult rat, during the first and the second introduction, respectively. Social recognition is determined to be present, if the test subject spends significantly less time investigating the familiar juvenile in the reintroduction test period. In this case, the SRR value is significantly lower than 0.5. A recognition ratio of 0.5 or above indicates no retention of social memory, meaning that the adult failed to recognize the acquaintance juvenile. The experiment was conducted and analyzed by a researcher that was blind with respect to the treatment groups. Rats were evaluated in a balanced design so that animals from each group were tested randomly during the test.

2.8. Spatial memory in the Morris water maze test

A circular tank of 160 cm in diameter and 60 cm in height was placed in a dimly lit room, filled with water (21 °C) up to 20 cm from the top, and virtually divided into 4 quadrants. Cues for visual orientation were placed in close proximity to the tank. A circular escape platform (10 cm in diameter) was immersed 1.5 cm under the water surface at the center of one of the quadrants (the training quadrant). The quadrants not hosting the platform served as starting positions. A video camera connected to a computerized tracking system (Ethovision 3.1, Noldus IT, Wageningen, The Netherlands) was placed above the tank for recording. The latency time to locate the platform, during reference memory training, and time spent in a virtual circle (60 cm in diameter with the center in the original platform location) during probe test were observed.

Before training, the animals (male Wistar rats) were handled 2 minutes daily for 5 days. The reference memory training, aimed to locate the platform, included 3 consecutive 90-second swims per day for 3 days. Each trial started with the rat being gently placed in the water, facing the wall of the tank, in the quadrants not hosting the platform. The starting position differed for each trial but was identical for all rats. Rats that did not find the platform were guided to the platform and given a latency score of 90 seconds. After each trial, the rats were allowed 20 seconds of orientation time on the platform and then removed from the pool for an intertrial period of 20 seconds. The mean latency was determined during each training session. On the first 2 days immediately after training, animals were given a subcutaneous injection of either NL100 (5 mg/kg; n = 12) in concentrations 5 mg/mL or saline (n = 12) (Fig. 4A). To evaluate long-term memory, a 60-second probe test was performed 24 hours

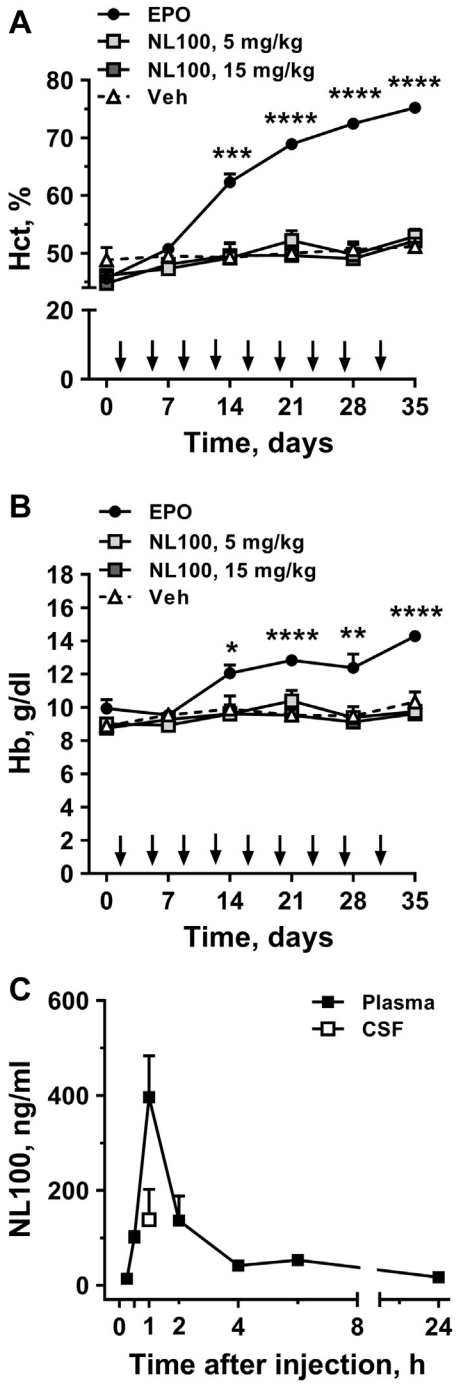

Fig. 2. EPO-mimetic peptide NL100 does not stimulate hematopoiesis in vivo. Male Wistar rats (n = 6 per group) were treated s.c. with EPO (5 μg/mL), NL100 (5 mg/kg or 15 mg/kg), or vehicle biweekly for 5 weeks (9 injections in total, indicated with arrows). (A) Hematocrit (Hct) and (B) hemoglobin levels (Hb) were measured in blood samples taken once per week for 6 weeks. The first samples at day 0 were collected before the stimulation. One-way ANOVA followed by Dunnett's multiple comparisons test. $^{*}p < 0.05$; $^{**}p < 0.01$; $^{***}p < 0.001$; $^{****}p < 0.0001$, EPO versus vehicle. (C) Time-course of NL100 plasma concentration and detection of the peptide in CSF. Male Wistar rats (n = 4 per group) received a single s.c. injection of NL100 (5 mg/kg) and blood samples were collected at 15 minutes, 30 minutes, 1 hour, 2 hours, 4 hours, 6 hours, and 24 hours, whereas CSF samples were collected at 1 hour after the administration. The concentration of NL100 in biological liquids was estimated by competitive ELISA. Abbreviations: EPO, erythropoietin; Hb, hemoglobin; Hct, hematocrit; CSF, cerebrospinal fluid.

and 1 week after the last reference memory training session. The platform was removed, and the animals started to swim from a position in a quadrant opposite (24 hours) or adjacent (7 days) to the original platform quadrant. At the end of the probe trial, the animal was guided to the reintroduced platform and allowed to stay there for 20 seconds. Subsequently, after the 24-hour probe trial, the animal was given a single relearning trial, under conditions identical to reference memory training, to counteract memory extinction. The experimenter conducting behavior scoring and data analysis was blinded to treatment conditions and the animals were randomly assigned to their groups.

2.9. Pilocarpine-induced status epilepticus

All injected solutions were prepared in sterile saline (0.9% w/v). At weaning (postnatal day 20 (P20)), Sprague-Dawley male rat pups were first injected i.p. with lithium chloride (127 mg/kg; Sigma-Aldrich), to decrease the dose of pilocarpine needed to trigger SE. Scopolamine methylnitrate (1 mg/kg; Sigma-Aldrich) was injected s.c. 18 hours later, to alleviate peripheral cholinergic adverse side effects. Pilocarpine hydrochloride (25 mg/kg; Sigma-Aldrich) was injected i.p. 30 minutes later, to induce SE. After 30 minutes of continuous behavioral SE, diazepam (Valium, Roche) was injected i.p. at 10 mg/kg, to promote survival and initiate cessation of behavioral seizures, that completely stopped after a second s.c. injection of diazepam, given 90 minutes later at the dose of 5 mg/kg. The rats were placed on a heated pad, under continuous observation, until they recovered from sedation. After recovery, the rats were returned to the nursing mother until P23. Control rats only received saline injections. All rats were then housed in groups of 10 and weighed daily, during the 5 following days, to control for food intake, and then twice weekly, until the end of experiment (3 weeks after SE). The rats, which did not increase in body weight on the second day after SE, were sacrificed with a lethal dose of dolethal (1.5 mL, i.p.; Vétoquinol, France).

2.10. Acute slice preparation and whole cell recordings

At P28-38, Sprague-Dawley rats were anesthetized with isoflurane, the forebrain was removed and placed in ice cold standard artificial cerebrospinal fluid (ACSF), consisting of (in mM) 124 NaCl, 5 KCl, 1.25 Na_2HPO_4, 2 $MgSO_4$, 2 $CaCl_2$, 26 $NaHCO_3$, supplemented with 10 D-glucose, and bubbled with 95% O_2 and 5% CO_2. Hippocampal transverse slices were cut into 350-μm-thick sections, using a vibratome (Leica VT1000S), and incubated in ACSF at room temperature for at least 1 hour, before the transfer to the recording chamber. The ACSF used for perfusion was supplemented with picrotoxin (100 μM; Sigma-Aldrich) to block GABA-A receptors and therefore to facilitate the induction of NMDA receptor–dependent LTP. CA1 pyramidal cells were visualized with a Zeiss Axioskop 2, equipped with a ×40 objective, using infrared video microscopy and differential interference contrast optics. Whole-cell recordings from pyramidal neurons in the CA1 layer were obtained with patch electrodes, which were filled with a solution containing (in mM) 120 potassium gluconate, 20 KCl, 0.2 EGTA, 2 $MgCl_2$, 10 HEPES, 4 Na_2ATP, 0.3 Tris-GTP, and 14 mM phosphocreatine (pH 7.3, adjusted with KOH). NL100 was applied in the bath of the hippocampal slices at 1 μM. Electrode resistances ranged from 3 to 5 MΩ. Series resistance was continually monitored, and experiments were discarded if it changed by >20%.

Capillary glass pipettes filled with ACSF and connected to an Iso-Flex stimulus isolation unit (A.M.P.I.) were placed in stratum radiatum, to evoke excitatory postsynaptic potentials (EPSPs) in CA1 pyramidal neurons. Cells were held at −70 mV to record EPSPs, and the stimulation strength was set to evoke EPSPs between 5 and 8 mV. To examine membrane excitability, cells were injected with

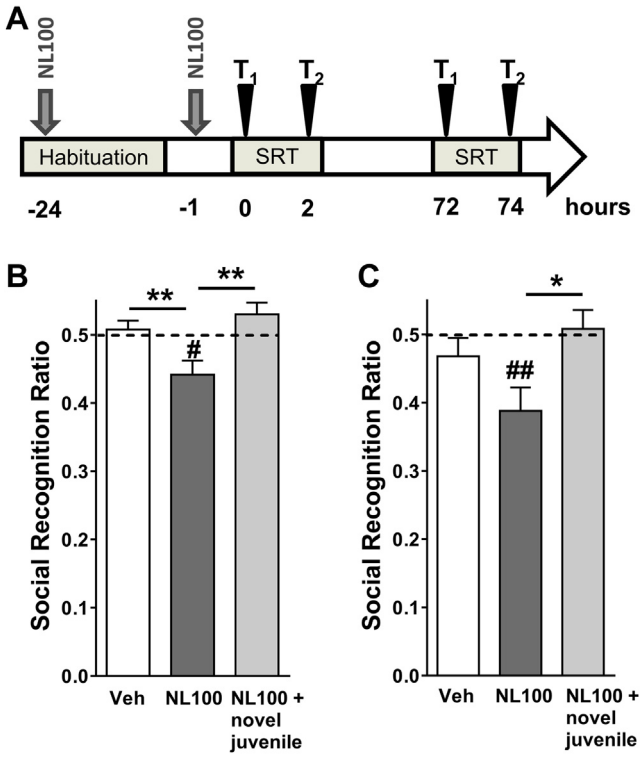

Fig. 3. The effect of NL100 on short-term retention of social memory. (A) Timeline of the experimental paradigm. Adult male Wistar rats were treated s.c. with NL100 (5 mg/kg) or vehicle (1 mL/kg), 24 hours and 1 hour before social memory evaluation (gray arrows); the time for performing the social recognition test (SRT) is indicated (black arrowheads). The juvenile rat was reintroduced with an intertrial interval of 2 hours. Quantification of the social recognition ratio at 1 hour (B) and 24 hours (C) after last vehicle/peptide administration. An unfamiliar juvenile was presented during the test trial, to control that the mnemonic effect of NL100 was specific to memory processes (light gray column). The data are expressed as mean ± SEM (n = 12 per group). $^{*}p < 0.05$; $^{**}p < 0.01$, compared with control (one-way ANOVA, followed by Newman-Keuls post hoc test); $\#p < 0.05$; $\#\#p < 0.01$, compared with the hypothetical value 0.5 (one-sample *t*-test).

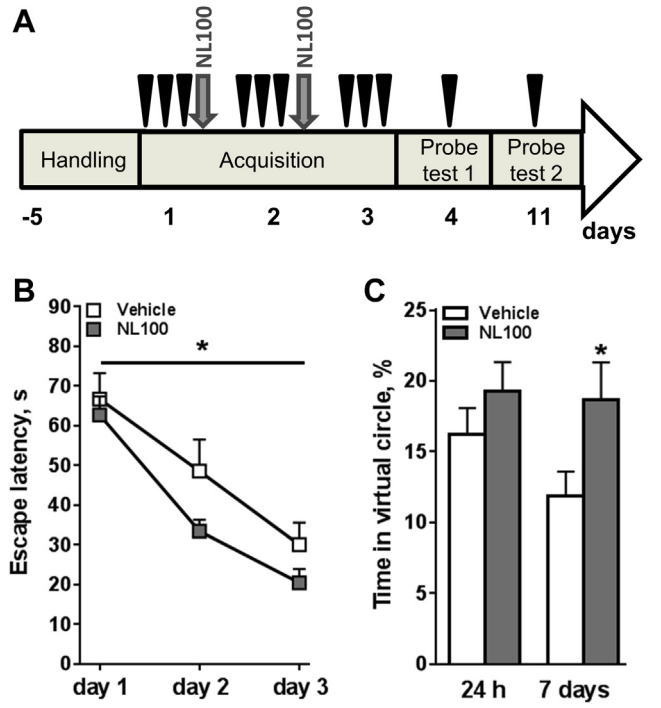

Fig. 4. The effect of NL100 on spatial learning and memory in the Morris water maze. (A) Timeline of the experimental paradigm. Male Wistar rats were treated s.c. with NL100 (5 mg/kg) or vehicle (1 mL/kg) after first and second training day (gray arrows); the time for introducing animals to the arena is indicated (black arrowheads). The graphs show the escape latency time to reach the hidden platform, during reference memory training (B), and the percentage of time spent in the virtual circle around platform zone, during the probe trials (C). After 7 days, vehicle- but not NL100-treated rats showed decrease in time spent in the circle ($p = 0.0578$). The data are expressed as mean ± SEM ($n = 12$ per group). $^{*}p < 0.05$, (two-way ANOVA, reference memory training); $^{*}p < 0.05$ (unpaired *t*-test, probe trial, compared to vehicle-treated rats at day 7).

250 ms depolarizing current pulses ranging from 50 to 400 pA at 50 pA increments and an intertrial interval of 5 seconds. For each neuron, this protocol was repeated twice, and the number of action potentials fired at each step was averaged. The paired-pulse facilitation (PPF) was examined by applying stimulus pairs at varying intervals. Electrical stimuli were applied at 0.05 Hz. The amplitudes of the responses were measured from digital averaging of 6 consecutive responses. LTP was induced by the theta burst pairing protocol, which consisted of EPSPs paired with single back-propagating action potentials (b-APs), timed so that the b-AP (~ 15 ms delay) occurred at the peak of the EPSPs, as measured in the soma. A single burst contained 5 pairs delivered at 100 Hz and 10 bursts were delivered at 5 Hz per sweep. Three sweeps were delivered at 10-second intervals for a total of 30 bursts (150 b-AP-EPSP pairs). The b-APs were elicited by direct somatic current injection (1 ms, 1–2 nA). This induction protocol was always applied within 20 minutes of achieving whole-cell configuration, to avoid "washout" of LTP.

2.11. Electrophysiological data acquisition and analysis

EPSPs and action potentials were recorded in whole-cell current clamp (Multiclamp 700B, Molecular Devices), filtered at 5 kHz, and digitized at 10 kHz (Digidata 1440A, Molecular Devices). Data were acquired and analyzed, using pClamp 10 software (Molecular Devices). To generate LTP summary time-course graphs, individual experiments were normalized to the baseline and 3 consecutive responses were averaged to generate 1-minute bins. The binned time courses of all experiments within a group were then averaged to generate the final graphs. The magnitude of LTP was calculated, based on the normalized EPSP amplitudes 36–40 minutes after the end of the theta burst pairing protocol.

2.12. Amyloid β neurotoxicity model

Neurotoxicity was induced by intracerebroventricular (i.c.v.) injections of $A\beta_{25-35}$ polymerized peptide, essentially as previously described (Klementiev et al., 2007). Briefly, male Wistar rats were randomly assigned to 3 groups and injected with either the vehicle (sham-control group; n = 12) or $A\beta_{25-35}$ (3 mg/mL; $A\beta_{25-35}$ alone; n = 10, and $A\beta_{25-35}$/NL100 groups; n = 11) in a final volume of 8 μL per rat under anesthesia (Hypnorm/midazolam; 0.3 mL/100 g animal, i.p.). The injection coordinates were as follows: 1 mm posterior to bregma; 1.5 mm lateral to the sagittal suture; 4.1 mm beneath the surface of the brain. Correct i.c.v. injection was verified by histological examination of the brain. NL100 (5 mg/kg, 5 mg/mL) was administered s.c. for 5 consecutive times starting from day 7 after $A\beta_{25-35}$ injection with 3-day intervals, following the previously established scheme with small modifications (Klementiev et al., 2014). The social recognition test was performed on day 21 after $A\beta_{25-35}$ injection (Fig. 5A), as described previously. At the day 28 after $A\beta_{25-35}$ injection, rats were sacrificed by an i.p. injection of pentobarbital (200 mg/kg), perfused transcardially with saline, followed by 4% (v/v) formaldehyde in PBS, and brain tissues were collected for histology.

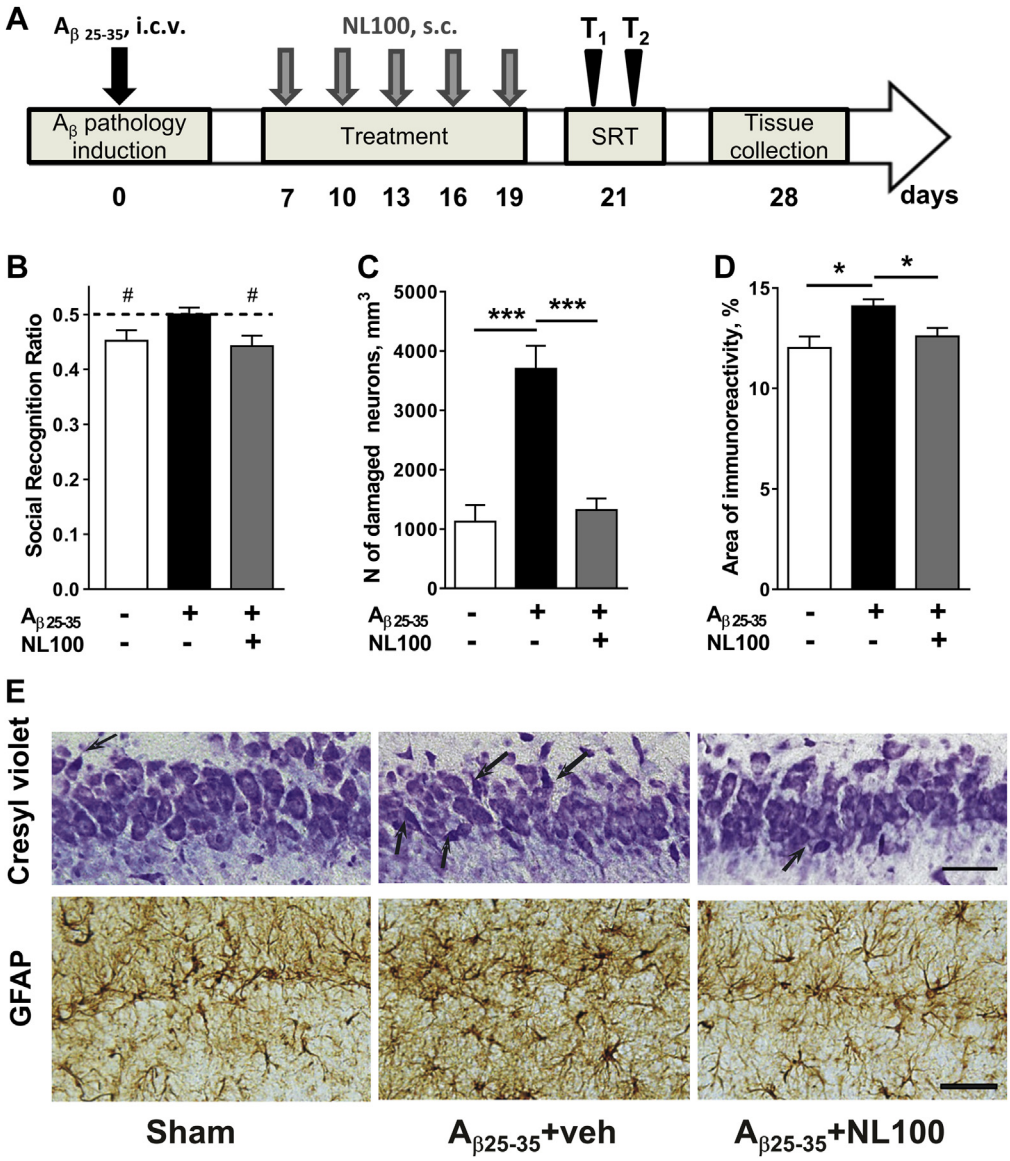

Fig. 5. NL100 improves memory and decreases hippocampal neuronal damage and gliosis in Aβ_{25-35} toxicity rat model. (A) Timeline of the experimental paradigm showing the time frame of Aβ_{25-35} i.c.v. injection (black arrow), 5 sequel treatments with NL100 peptide (5 mg/kg, s.c.; gray arrows), the memory assessment by social recognition test (SRT) at week 3 (black arrowheads), and the tissue collection at week 4 (day 28). (B) Quantification of social recognition ratio (SRR) on day 21 for sham-control rats, and rats injected with either Aβ_{25-35} alone or Aβ_{25-35} followed by NL100 treatment (male Wistar rats). The level of SRR of 0.5 indicates no memory (dashed line). Both sham-control and Aβ_{25-35}+NL100-treated rats had significantly lower ratios than 0.5 ($^{\#}p < 0.01$; one-way ANOVA), while rats treated solely with Aβ_{25-35} had not. Number of animals per group: 12/11/11 in sham/Aβ_{25-35}/Aβ_{25-35}+NL100. (C, D) The effect of NL100 treatment on number of damaged neurons (C) and astrogliosis (D) within the CA3 region of the hippocampus. Number of neurons was evaluated with unbiased stereological approach. Results are presented as mean ± SEM. $^{*}p < 0.05$, $^{***}p < 0.001$, one-way ANOVA, followed by Tukey's multiple comparison post hoc test. Number of animals per group: 7/9/7 in sham/Aβ_{25-35}/Aβ_{25-35}+NL100, respectively. (E) Representative micrographs showing either the histological staining with cresyl violet (top row) or GFAP immunoreactivity (bottom row) within the hippocampal formation of control for Aβ_{25-35}-treated rats and Aβ_{25-35}-injected NL100-treated rats, respectively. Neurons with pyknotic, smaller intensively stained nuclei are depicted with arrows. Bars are 50 μm for both cresyl violet and GFAP-positive images. Abbreviations: Aβ, amyloid beta; GFAP, glial fibrillary acidic protein; i.c.v., intracerebroventricular injection. (For interpretation of the references to color in this figure legend, the reader is referred to the Web version of this article.)

2.13. Histological and immunohistochemical analysis

Formalin-fixed frozen free-floating serial brain sections (80 μm) were stained with cresyl violet, to quantify the number of damaged neurons. The total number of neurons and the volume of the CA3 area of the dorsal hippocampus (from −2.3 mm to −4.52 mm in the coronal plane relative to Bregma) were measured by examining 8 sections per structure using Olympus BX50 microscope equipped with the C-5050 digital camera (Olympus Denmark A/S, Ballerup, Denmark). The volume of the brain regions was estimated, using Cavalieri's principle. Estimation of the total number of neurons was obtained with an optical disector (Gundersen et al., 1988), essentially as described (Enevoldsen et al., 2012). Stereological counting was performed with the CAST-GRID software (Olympus Denmark A/S). The observers blinded to the study groups accomplished all histological assessments.

Immunohistochemistry was performed on free-floating 40-μm sagittal sections, according to standard procedures (Enevoldsen et al., 2012), using anti-GFAP mouse polyclonal antibody (diluted 1:800) (DakoCytomation, Glostrup, Denmark). Immunoreactivity was quantified on the basis of the average brightness. Between 20 and 25 images, covering the whole area of interest, were captured

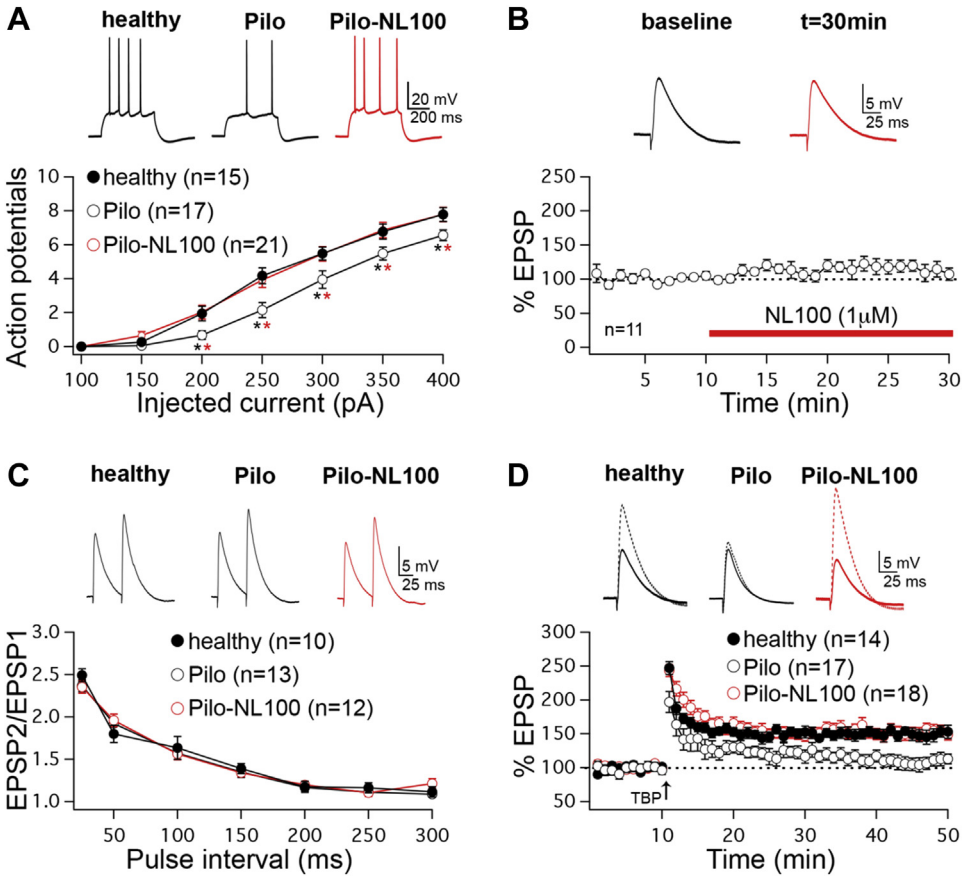

Fig. 6. Hippocampal neuronal excitability and LTP are attenuated following Pilo-SE and rescued by NL100 peptide in male Sprague-Dawley rats. (A) Plot of evoked spike rates versus current magnitudes (I/O curve) of pyramidal cells in slices of healthy rats (black circles) and in slices from rats subjected to Pilo-SE and perfused either with NL100-free ACSF (white circles) or NL100 (red circles). The top traces represent the action potential firing evoked by a 250 pA/550 ms current injection in pyramidal neurons from healthy rats and 2 other groups. $^{*}p < 0.05$. (B) Time graph showing EPSP amplitudes (n = 11), before and after NL100 bath application (bar). Data were normalized to a baseline recorded during the last 5 minutes before NL100 washing. The top traces show EPSPs before and after (30 minutes) NL100 application. (C) Summary diagram of the PPF ratio at the indicated stimulus intervals, recorded from same slices of the 3 different groups. The top traces show facilitation at 250 ms interpulse intervals. (D) Time course of EPSP amplitudes before and after TBP (indicated by arrow), in hippocampal slices from same 3 different groups. The top traces show EPSPs before and after (dashed) LTP induction (t = 50 minutes). In this and all subsequent figures, summary data are presented as mean ± SEM and numbers between brackets indicate the number of cells. Abbreviations: ACSF, artificial cerebrospinal fluid; EPSP, excitatory postsynaptic potential; LTP, long-term potentiation; PPF, paired-pulse facilitation; Pilo, pilocarpine; TBP, theta burst pairing. (For interpretation of the references to color in this figure legend, the reader is referred to the Web version of this article.)

from 3 sections per animal. The images were adjusted to the same threshold level for each staining, defined so the immune signal could be unambiguously identified. The amount of antigen was expressed as the average percentage of the image area occupied by positive immunoreactivity.

2.14. Statistical analysis

Data analysis was performed using GraphPad Prism version 4.02 (GraphPad, San Diego, CA). The cell culture data (2.3 neurite outgrowth; 2.4 neuronal survival; Fig. 1C–E) and the biochemical data (2.6 hematopoietic activity; Fig. 2A–B, Suppl. Fig. S1 A-B) were analyzed by repeated-measures one-way analysis of variance (ANOVA), followed by Dunnett's post hoc tests for multiple comparisons versus control. The in vivo test data were analyzed using one-sample *t*-test or one-way ANOVA followed by the Newman-Keuls post hoc tests (2.7 social recognition test; Figs. 3B–C, 5B) and two-way ANOVA for examination of differences in effect between treatment groups over acquisition training time, and Student's *t*-test for comparisons between groups in the probe test trials (2.8 Morris water maze test; Fig. 4B–C). Histological data analysis was performed using one-way ANOVA, followed by the Newman-Keuls post hoc tests (2.13 histological and immunohistochemical analysis; Fig. 5C–D). Data from electrophysiology experiments (2.11 electrophysiological data analysis) were analyzed using the paired Student's *t*-tests to determine significance of data in the same pathway, the Mann–Whitney *U* test to determine significance between groups of data, and the repeated-measures ANOVA to analyze the firing frequency and PPF over the time points indicated (Fig. 6 and Fig. S2). Results are expressed as mean ± SEM. Values of $p < 0.05$ were considered statistically significant.

3. Results

3.1. NL100 binds to the EPO receptor and promotes neurite outgrowth and neuronal survival

Structurally, human EPO protein has a globular form consisting of up-up-down-down oriented 4 α-helices denominated A, B, C, and D. EPO interacts with 2 EPOR subunits simultaneously, via 2 distinct binding sites located on the EPO surface: the high affinity site 1 involving the amino acid from helices A, B, D, and AB loop; and the low affinity binding site 2 involving the amino acids from helices A and C (Syed et al., 1998). The 12-mer motif $_{127}$SGLRSLTTLLRA$_{138}$ (Uniprot P01588), termed NL100, is located in C-terminal side of EPO helix C (Fig. 1A top; marked in green) and comprises 4 out of 16

amino acids, whose side chains are involved in the formation of binding site 2 in the EPO:$EPOR_2$ complex (Syed et al., 1998). Sequence alignment revealed the NL100 motif to be strongly conserved across mammalian species (Fig. 1A; bottom). We applied real-time SPR approach to test the binding of NL100 to EPOR. First, the functionality of immobilized EPOR was verified by binding to its cognate ligand, recombinant human EPO (data not shown). Furthermore, SPR measurements showed that NL100 dose-dependently bound to immobilized EPOR with apparent K_D value 4.2 ± 0.8 μM (Fig. 1B).

Treatment with NL100 improved the survival of hippocampal neurons challenged with either $A\beta_{25-35}$ (Fig. 1C; $p < 0.05$) or oxidative stress (H_2O_2, Fig. 1D; $p < 0.001$). NL100 showed single effective concentration (3 μM) in $A\beta_{25-35}$ in vitro test and broader effective concentrations in oxidative stress (0.3–9 μM). The magnitude of the prosurvival effect of NL100 at the optimal dose (1–2 μM) is comparable to that of EPO (14 nM), used as a positive control in both in vitro survival models (Fig. 1C and D). The neurotrophic potential of EPO is well described (Morishita et al., 1997; Siren et al., 2001). Neuritogenesis is an early morphological event accompanying neuronal differentiation, facilitating the formation of mature axons and dendrites, harboring the synaptic cell-to-cell contacts underlying some types of memory formation (Meldolesi, 2011). Thus, the potential neuritogenic activity of the NL100 peptide was evaluated by in vitro functional tests. Stimulation of primary hippocampal neurons with NL100 peptide significantly promoted neurite outgrowth, with effective concentrations ranging from 2.9 to 9 μM (Fig. 1E; $p < 0.01$).

Collectively, the short NL100 peptide binds to EPOR within μM affinity range and is a potent neurotrophic and prosurvival agent, with an efficacy similar to that of EPO, but with approximately 70-fold lower potency.

3.2. NL100 does not affect hematopoiesis and crosses the BBB

The segregation of hematopoietic and neurotrophic activities has recently been confirmed for EPO splice isoform, EV-3 (Bonnas et al., 2017), and for a number of EPO derivates and peptide mimetics, including Epotris and Epobis peptides (Dmytriyeva et al., 2016; Pankratova et al., 2010). Thus, we next investigated the effect of the NL100 peptide on hematopoiesis during long-term treatment. In contrast to stimulation with EPO (5 μg/kg), the repetitive long-term treatment of rats with NL100 in dose either 5 mg/kg or 15 mg/kg s.c. for 4 weeks did not increase hematocrit or hemoglobin levels (Fig. 2A and B). Simultaneous long-term treatment of mice with high dose of NL100 (14 mg/kg) twice a week for 5 weeks also did not affect aforementioned blood parameters (Fig. S1), indicating that the NL100 peptide does not stimulate hematopoiesis in vivo.

Systemically administered EPO has been shown to cross BBB in rats and humans (Ehrenreich et al., 2004; Xenocostas et al., 2005). Therefore, we next investigated whether peripherally administered NL100 would be detectable in rat CSF. We observed that plasma concentration of bNL100 peaked 1 hour after single s.c. injection of the peptide (5 mg/kg) and then rapidly decreased but remained detectable for at least 24 hours. CSF samples collected at 1 hour after the administration revealed NL100 at a concentration of 139 ng/mL (Fig. 2C), which is approximately 3 times lower than the plasma concentration at the same time point, thus indicating that NL100 crosses the BBB.

3.3. NL100 stimulates social recognition memory

EPO has been demonstrated to have memory enhancing effects under pathological conditions (Kumral et al., 2004; Lee et al., 2012), in healthy volunteers (Miskowiak et al., 2007), and preclinically in mice (Adamcio et al., 2008; El-Kordi et al., 2009). First, we investigated whether treatment with the EPO mimetic peptide NL100 could improve cognitive functions under normal physiological conditions. We analyzed the effect of NL100 on short-term social recognition memory, which has been suggested to predominantly involve the dorsal hippocampus, a region affected by sclerosis during AD pathology, and the basolateral amygdala (Garrido Zinn et al., 2016). Rats were treated with NL100 at 24 hours and 1 hour, before being shortly presented to an unfamiliar juvenile of same species, strain, and gender (Fig. 3A). Two hours later, test rats were reintroduced to the same juvenile rat. The difference in inquisitiveness behaviors between the first and second encounter with the juvenile was taken as a measure of familiarity and short-term recognition memory. Rats treated with NL100 demonstrated a clear decrease in SRR ($p < 0.01$), which is indicative of enhanced social discrimination memory. To exclude the potential influence from nonmnemonic effects, it was demonstrated that the rats exhibited normal inquisitiveness toward an unfamiliar second juvenile rat in a subsequent session (Fig. 3B; $p < 0.01$). Interestingly, the improved memory traces were still apparent 72 hours after the last injection of the peptide (Fig. 3C; $p < 0.05$). Thus, NL100 improves short-term memory under physiological conditions.

3.4. NL100 improves spatial memory in the Morris water maze

We next investigated the effect of NL100 on spatial memory in the Morris water maze test (Fig. 4A). NL100 treated rats were faster at locating the escape platform, during the total span of the 3-day reference memory trials, which indicates improved learning and memory (Fig. 4B; $p < 0.05$). Moreover, NL100 treatment also resulted in increased time spent in the concentric vicinity around the platform location, indicating improved spatial memory, manifesting on day 7 when compared to vehicle-treated animals (Fig. 4C; $p < 0.05$). Thus, coherently to the findings in the social recognition memory test, NL100 improved both short- and long-term spatial memory.

3.5. NL100 counteracts memory deficits and neuropathology induced by $A\beta_{25-35}$

It has been previously demonstrated that treatment with EPO or nonerythropoietic EPO derivates enhances memory in transgenic and nontransgenic animal models of AD (Arabpoor et al., 2012; Armand-Ugon et al., 2015; Maurice et al., 2013; Rodriguez Cruz et al., 2017). We, therefore, investigated the effect of EPO mimetic NL100 in the established model of $A\beta_{25-35}$-induced cognitive impairment and neuropathology (Klementiev et al., 2007; Zussy et al., 2011). The SRR index for rats treated with $A\beta_{25-35}$ alone ($n = 10$) was at the level of 0.5, whereas the sham-operated control group ($n=12$) was significantly below the ratio level of the $A\beta_{25-35}$ group (Fig. 5B; $p < 0.05$). This indicates that, in contrast to sham controls, rats receiving the i.c.v. injection of the $A\beta_{25-35}$ peptide were unable to recognize the juvenile rat, during the second presentation round. Thus, in accordance with the previously established model (Klementiev et al., 2007), a single treatment with the $A\beta_{25-35}$ peptide caused short-term memory impairment (3 weeks after the pathology induction). Repeated treatment with NL100, initiated after the Aβ challenge (Fig. 5A), counteracted the cognitive deficits developed at day 21, as demonstrated by a significant decrease in SRR level (Fig. 5B; $p < 0.05$; $n = 11$).

At the conclusion of the experiment on day 28, the degeneration of pyramidal neurons within the CA3 region of hippocampal formation was analyzed, using an unbiased stereological approach. The results showed that a single i.c.v. injection of $A\beta_{25-35}$ peptide significantly increases the number of damaged neurons within the

CA3 region (Fig. 5C; $p < 0.001$), confirming the previous observations (Corbett et al., 2013; Zussy et al., 2011). The treatment with the NL100 peptide reversed neuronal damage induced by Aβ (Fig. 5C and E; $p < 0.001$).

Given that $A\beta_{25-35}$-induced neurotoxicity is associated with reactive cerebral and particularly hippocampal astrogliosis (Zussy et al., 2011), and because hippocampal astrocytes were previously shown to express EPOR (Nadam et al., 2007), we tested whether the treatment with NL100 could counteract Aβ-induced gliosis. By using GFAP-immunoreactivity, which is indicative of astrogliosis, we showed that treatment with $A\beta_{25-35}$ alone significantly increases GFAP-immunoreactivity (Fig. 5D, $p < 0.05$). At the end of 4th week after i.c.v. injection of $A\beta_{25-35}$, strongly labeled astrocytes with pronounced hypertrophy, a typical morphology of their activated state, were observed within CA3 region of the hippocampal formation (Fig. 5E). The treatment with the NL100 peptide significantly decreased GFAP-immunoreactivity in the hippocampus, compared to rats treated with $A\beta_{25-35}$ alone (Fig. 5D and E; $p < 0.05$). There was a high correlation between the levels of social memory (SRR) and GFAP immunoreactivity ($p = 0.0068$; $r_s = -0.93$) and the number of damaged neurons and GFAP immunoreactivity ($p = 0.0135$; $r_s = 0.5179$). Thus, NL100 prevented the development of memory deficit and neuropathological consequences of $A\beta_{25-35}$-induced neurotoxicity.

3.6. NL100 rescues hippocampal intrinsic excitability and LTP deficits following pilocarpine-induced status epilepticus

Although a wide range of neuropsychological deficits may follow SE, cognitive impairment and memory deficits are a major common problem in patients with epilepsy, especially in patients with temporal lobe epilepsy (TLE) (McCagh et al., 2009) consistent with data from animal models (Groticke et al., 2007). Because LTP, a form of synaptic plasticity that is believed to reflect processes of learning and memory formation in hippocampus (Bliss and Collingridge, 1993), is significantly abolished in hippocampal neurons in both humans with epilepsy and animal models of epilepsy, the impairment of LTP has been considered an important cellular mechanism underlying learning deficits in epilepsy (Cain et al., 1993). Therefore, the pilocarpine-induced experimental TLE model was used to examine the effect of NL100 on hippocampal LTP.

Recently, it was shown that EPO enhanced synaptic plasticity and memory functions in the hippocampus of healthy animals (Adamcio et al., 2008; Kamal et al., 2011; Maiese et al., 2012) and in the brain of injured animals (Esmaeili Tazangi et al., 2015; Jun et al., 2009). We have also previously demonstrated that hippocampal-dependent spatial memory and LTP, a candidate mechanism for learning and memory, were altered following pilocarpine-induced status epilepticus (Pilo-SE) (Fares et al., 2013). We, therefore, investigated whether application of NL100 (1 μM) could improve neuronal excitability, synaptic transmission, and plasticity in rats subjected to Pilo-SE.

Because neuronal excitability has been associated with synaptic plasticity, learning, and memory (Belmeguenai et al., 2010; D'Amelio and Rossini, 2012), we first examined the effects of NL100 on intrinsic excitability of pyramidal neurons in the hippocampal CA1 region, an area critically involved in memory formation. Evoked by a current of 200–400 pA amplitudes, the firing frequency of neurons was significantly decreased in slices, prepared from rats subjected to Pilo-SE, when compared to the healthy animals (Fig. 6A; $p < 0.05$). Moreover, perfusion of slices, prepared from rats subjected to Pilo-SE, with NL100 resulted in an increased action potential firing, compared to Pilo-SE slices perfused with NL100-free ACSF (Fig. 6A; $p < 0.05$). At current amplitudes above 200 pA, the average frequency of firing was significantly greater than the average Pilo-SE frequency.

We then investigated whether NL100 improved hippocampal synaptic transmission in slices, prepared from rats subjected to Pilo-SE. Bath application of NL100 had no significant effect on the amplitude of EPSPs (114.0% ± 10.1% of baseline; t = 26–30 minutes; Fig. 6B; $p = 0.16$). To examine if Pilo-SEs resulted in presynaptic changes, we measured PPF. PPF is a presynaptic form of short-term plasticity and is based on an increased release probability at the second pulse, due to residual presynaptic calcium from the first pulse. We found no significant differences in the PPF ratios of Pilo-SE rats, as compared to healthy rats, at all time intervals measured (Fig. 6C). Similarly, the PPF ratios were unaffected by bath application of NL100, suggesting that transmitter release was not impaired (Fig. 6C).

We recently revealed that hippocampal LTP is altered following Pilo-SE (Fares et al., 2013). To confirm these results, we examined LTP induction in slices prepared from healthy rats and animals subjected to Pilo-SE. Although control neurons in slices prepared from healthy animals exhibited robust LTP (147.6% ± 8.5% of baseline; t = 46–50 minutes; Fig. 6D; $p < 0.001$), LTP was blocked in slices prepared from rats subjected to Pilo-SE (109.6% ± 8.7%; t = 46–50 minutes; Fig. 6D; $p = 0.13$). The difference in LTP amplitude between these 2 groups of rats was highly significant ($p < 0.001$). We next investigated whether NL100 perfusion could reverse Pilo-SE-induced LTP deficits. We showed that NL100 bath application significantly enhanced LTP induction at the early (205.1% ± 9.5% of baseline; t = 11–15 minutes; Fig. 6D; $p < 0.001$) and the late phase (153.2% ± 8.5% of baseline; t = 46–50 minutes; Fig. 6D; $p < 0.001$), compared to the Pilo-SE slices perfused with NL100-free ACSF ($p = 0.002$; t = 11–15 minutes and $p < 0.001$; t = 46–50 minutes). Interestingly, LTP magnitude measured in Pilo-SE slices was similar to that of healthy rats ($p = 0.14$; t = 11–15 minutes and $p = 0.98$; t = 46–50 minutes). Altogether, our data reveal that impairment of hippocampal neuronal excitability and LTP during epileptogenesis can be rescued by NL100 treatment.

3.7. NL100 did not affect hippocampal neuronal excitability, synaptic transmission, and plasticity in healthy rats

Recently, it was revealed that EPO treatment enhances synaptic plasticity in healthy mouse hippocampal slices (Adamcio et al., 2008; Kamal et al., 2011; Maiese et al., 2012). We, therefore, investigated whether the EPO-mimetic peptide, NL100, could increase neuronal excitability, synaptic transmission, and plasticity in the hippocampus of healthy rats. We found that application of NL100 to healthy slices did not affect action potential firing (Fig. S2A). At each current amplitude, the average frequency of firing was similar to the healthy slices perfused with NL100-free ACSF (Fig. S2A). As in Pilo-SE animals, application of NL100 to healthy slices had no significant effect on the amplitude of EPSPs (108.04% ± 4.17% of baseline; t = 26–30 minutes; Fig. S2B; p=0.07) and PPF ratios (Fig. S2C). While application of NL100 did not affect the late phase of LTP (152.9% ± 9.8% of baseline; t = 46–50 minutes; Fig. S2D; $p < 0.001$) in healthy slices ($p = 0.93$), early phase of LTP was enhanced (216.5% ± 8.6%; t = 11–15 minutes; Fig. S2D; $p < 0.001$) compared to the healthy slices perfused with NL100-free ($p = 0.009$; t = 11–15 minutes and $p = 0.93$; t = 46–50 minutes). These findings demonstrate that NL100 does not affect hippocampal neuronal excitability and synaptic transmission in healthy rats. These results also reveal that NL100 does not affect late phase of hippocampal LTP in healthy rats but increases short-term phase of the potentiation.

4. Discussion

Here we demonstrate that a novel EPO-derived peptide NL100 possesses the ability of its parent protein to promote neurite outgrowth and improve neuronal survival in vitro. Applied systemically, the NL100 peptide crosses BBB and improves short- and long-term memory in healthy rats and rescues social recognition deficits induced by i.c.v. injection of $A\beta_{25-35}$ peptide, a rat model of AD (Klementiev et al., 2007; Maurice et al., 2013), and this effect is associated with reduced gliosis and decreased number of damaged neurons in the hippocampus. The ex vivo applied NL100 counteracts the pilocarpine-induced impaired excitability and LTP deficit in hippocampal slices, suggesting that the peptide may directly impact synaptic plasticity that provides a plausible linkage to the mnemonic effects of NL100. Moreover, the positive effect of NL100 on memory was not accompanied by increased hematopoiesis because long-term consecutive systemic treatment with NL100 does not affect hematocrit and hemoglobin levels.

A number of neurodegenerative disorders, including AD, vascular dementia, and hippocampal sclerosis induced by temporal lobe epilepsy, are associated with progressive memory impairment and decline of cognitive functions, expressed mainly in the form of impaired executive and attention processes (Muller et al., 2009; Walsh and Selkoe, 2004). These neurodegenerative processes are accompanied by misbalanced expression of trophic factors (Benussi et al., 2017). Particularly for the EPO system, brains from AD patients and from mice with AD-like pathology showed decreased EPO and increased EPOR levels (Assaraf et al., 2007; Lourhmati et al., 2013). In addition, natural physiological conditions, such as aging, are also accompanied with declining memory (Buckner, 2004) and decreased expression of trophic factors, including EPO (Chung et al., 2004; Li et al., 2016a). Thus, it is conceivable that targeting the EPOR-mediated signaling could be a promising approach for development of drugs with neuroprotective and memory-improving characteristics.

The modest amount of currently available memory-improving drugs is, at least in part, related to the limited delivery and targeting of therapeutic molecules into the brain (Saunders et al., 1999). As such, the smaller-in-size peptides gain an advantage as potential CNS drug candidates because they are more prone to be carried over the BBB and into the brain compartments (Upadhyay, 2014). In this regard, the recent development of a number of neurotrophic EPO-mimetic peptides, by us and others (ARA290, Epotris, Epobis, JM4) with prominent CNS delivery characteristics, makes the small-in-size EPO mimetics feasible and promising drug candidates for treatment of neurodegenerative disorders. Similarly, in this study, we characterized the short NL100 dimeric peptide, which sequence motif partially covers the EPO-binding site to the receptor and mimics the neurotrophic potential of full-length EPO. However, the affinity of the NL100 peptide to the EPOR is in the micromolar range, which is somewhat low, and might be considered as a limiting factor for potential clinical application of this peptide. Nevertheless, results obtained with employment of several types of memory tests, such as social recognition and Morris water maze tests, combined with different regiments of the peptide treatment simultaneously validate the memory-enhancing effect of systemically applied NL100 in healthy and $A\beta_{25-35}$-challenged rats.

In addition to EPOR homodimer, the βc receptor was functionally linked to the EPOR more than 2 decades ago (Jubinsky et al., 1997). It has been suggested that this heteroreceptor system is responsible for tissue protective activity of EPO (Brines et al., 2004), but still the existence of this complex is controversial (Cheung Tung Shing et al., 2018). Within EPO tertiary structure, helix B was suggested to be involved in the interaction with the βc receptor (Brines et al., 2008). Because the motif of the NL100 peptide is derived from helix C of EPO, we suggest that the EPOR homodimer rather than the EPOR:βc heterocomplex mediates the neurotrophic activity of the peptide. However, we do not exclude the possibility that other yet-to-be-identified EPO neuroprotective receptors might be involved (Ostrowski and Heinrich, 2018).

Pharmacokinetic studies, performed with a longer isoform of the NL100-related peptide, that is, Epotris (Pankratova et al., 2010), and for another EPO-derived peptide, Epobis (Dmytriyeva et al., 2016), demonstrated that these peptides were both detected in blood plasma and the cerebrospinal fluid after s.c. injection—indicative of BBB crossing and CNS entrance. In line with previous studies, we showed that NL100, which has almost 3 times lower molecular weight than its longer isoform (2843.4 kD for NL100 vs. 9114.9 kD for Epotris), is capable of crossing the BBB and therefore might directly act on neuronal cells to improve memory in healthy and Aβ-induced pathology. In support of this, EPOR is shown to be expressed by variety of neuronal cell types (Lee et al., 2012; Nadam et al., 2007; Ott et al., 2015; Sanchez et al., 2009), and its expression is upregulated in response to injury and in AD pathological stages (Assaraf et al., 2007; Lourhmati et al., 2013; Nadam et al., 2007; Ott et al., 2015). Similarly in humans, the expression of the hippocampal EPOR is upregulated in chronic epilepsy patients (Ott et al., 2015). In addition, we recently demonstrated that optimal neuroprotection by EPO requires upregulation of EPOR in neurons, either through environmental enrichment or hypoxia (Sanchez et al., 2009). Thus, the observed improving effect of NL100 on neuronal excitability and LTP after pilo-SE, but not during basal conditions, suggests that the level of EPOR might be one of the critical parameters for its normalizing effect on LTP (Fig. 6). The observed LTP potentiation by NL100 is in line with previous findings, showing the potentiation of LTP followed by EPO stimulation (Adamcio et al., 2008).

Social recognition is important for initiation, development, and maintenance of social relationships. However, this type of activity is declining in age-related neurodegenerative disorders and particularly in AD patients, who face earlier-onset cognitive and social challenges (Belfort et al., 2018). The hippocampus is known to be involved in formation of social recognition memory in humans (Bediou et al., 2009) and rodents (Garrido Zinn et al., 2016; Kogan et al., 2000; Liu et al., 2017). The hippocampal neuronal loss and astrocyte hypertrophy are characteristic hallmarks for the AD phenotype and are assumed to contribute to AD-associated cognitive dysfunction (Simpson et al., 2010). Thus, in line with previous findings (Klementiev et al., 2007), we observed the degeneration of pyramidal neurons and an increase in astrocytic reactivity in the CA3 after i.c.v. injection of $A\beta_{25-35}$. Moreover, we found that the level of gliosis is correlated with decline in social recognition memory, supporting the previous results shown for AD patients (Simpson et al., 2010). Treatment with NL100 improves the social memory—related deficits in AD rats, probably via attenuation of neuronal damage and downregulation of astrogliosis (Fig. 5). Thus, the memory-enhancing effect and accompanied pathology-phenotype-improving effect of NL100 might, at least partially, be due to decreased astrogliosis and antiapoptotic effects. The latter is also corroborated by observed prosurvival effects of NL100 in the in vitro oxidative- and, to a less degree, in $A\beta_{25-35}$-induced toxicity models (Fig. 1C and D). Although, further experiments aimed to directly compare NL100 and EPO promnemonic effects in different paradigms would be required, the initial results showed that NL100 improves the memory acquisition and retention, as shown in both probe trial and hidden platform setups of the Morris water maze tests (Fig. 4), indicating the promnemonic effect of NL100 in intact brains.

Importantly, the beneficial effects of NL100 on cognitive functions could not be explained by its indirect action via increasing hemoglobin levels because this EPO-mimetic peptide has no

hematopoietic effect (Fig. 2). This finding is aligned with previous results showing that properly selected doses of EPO have beneficial effects on memory, without an accompanying increase in hemoglobin level (Miskowiak et al., 2007, 2008a). Coherently, an investigation on healthy volunteers, using functional neuroimaging, showed that a single dose of EPO versus placebo has a greater memory-related hippocampal response without changes in hematological parameters (Miskowiak et al., 2007). Apart from that, recent discovery in human samples of the naturally expressed nonhematopoietic splice variant of EPO, EV-3, with confirmed neuroprotective activities (Bonnas et al., 2017), further supports the neurotrophic and plasticity-improving effect of EPOR ligand(s), acting independently on hematopoiesis.

In summary, we here described a novel short nonhematopoietic EPO-derived peptide, NL100, as a neuroprotective substance, able to halter neurodegeneration and gliosis in the hippocampus with a procognitive effect in healthy rats and in an $A\beta_{25-35}$-induced AD-like pathology rat model. Taken together, this indicates that NL100 could be a potential candidate for development of new treatments for broad-spectrum neurodegenerative disorders and dementia.

Disclosure

All authors declare no conflicts of interest.

Acknowledgements

This work is dedicated to the memory of Prof. Vladimir Berezin, who passed away on the 14th of February 2016. Authors acknowledged Tatiana Novikova for help with stereological evaluation of histological images. This work was supported by fellowships from Velux Foundation to OD (00010310) and Lundbeck Foundation to SP (R83-A8113, R118-A11752 and R315-2018-3679).

Appendix A. Supplementary data

Supplementary data to this article can be found online at https://doi.org/10.1016/j.neurobiolaging.2019.05.003.

References

Adamcio, B., Sargin, D., Stradomska, A., Medrihan, L., Gertler, C., Theis, F., Zhang, M., Muller, M., Hassouna, I., Hannke, K., Sperling, S., Radyushkin, K., El-Kordi, A., Schulze, L., Ronnenberg, A., Wolf, F., Brose, N., Rhee, J.S., Zhang, W., Ehrenreich, H., 2008. Erythropoietin enhances hippocampal long-term potentiation and memory. BMC Biol. 6, 37.

Almaguer-Melian, W., Merceron-Martinez, D., Delgado-Ocana, S., Pavon-Fuentes, N., Ledon, N., Bergado, J.A., 2016. EPO induces changes in synaptic transmission and plasticity in the dentate gyrus of rats. Synapse 70, 240–252.

Arabpoor, Z., Hamidi, G., Rashidi, B., Shabrang, M., Alaei, H., Sharifi, M.R., Salami, M., Dolatabadi, H.R., Reisi, P., 2012. Erythropoietin improves neuronal proliferation in dentate gyrus of hippocampal formation in an animal model of Alzheimer's disease. Adv. Biomed. Res. 1, 50.

Armand-Ugon, M., Aso, E., Moreno, J., Riera-Codina, M., Sanchez, A., Vegas, E., Ferrer, I., 2015. Memory improvement in the AbetaPP/PS1 mouse model of familial Alzheimer's disease induced by carbamylated-erythropoietin is accompanied by modulation of synaptic genes. J. Alzheimers Dis. 45, 407–421.

Assaraf, M.I., Diaz, Z., Liberman, A., Miller Jr., W.H., Arvanitakis, Z., Li, Y., Bennett, D.A., Schipper, H.M., 2007. Brain erythropoietin receptor expression in Alzheimer disease and mild cognitive impairment. J. Neuropathol. Exp. Neurol. 66, 389–398.

Bahcekapili, N., Akgun-Dar, K., Albeniz, I., Kapucu, A., Kandil, A., Yagiz, O., Uzum, G., 2014. Erythropoietin pretreatment suppresses seizures and prevents the increase in inflammatory mediators during pentylenetetrazole-induced generalized seizures. Int. J. Neurosci. 124, 762–770.

Barichello, T., Simoes, L.R., Generoso, J.S., Sangiogo, G., Danielski, L.G., Florentino, D., Dominguini, D., Comim, C.M., Petronilho, F., Quevedo, J., 2014. Erythropoietin prevents cognitive impairment and oxidative parameters in Wistar rats subjected to pneumococcal meningitis. Transl Res. 163, 503–513.

Bediou, B., Ryff, I., Mercier, B., Milliery, M., Henaff, M.A., D'Amato, T., Bonnefoy, M., Vighetto, A., Krolak-Salmon, P., 2009. Impaired social cognition in mild Alzheimer disease. J. Geriatr. Psychiatry Neurol. 22, 130–140.

Belfort, T., Simoes, P., de Sousa, M.F.B., Santos, R.L., Barbeito, I., Torres, B., Dourado, M.C.N., 2018. The relationship between social cognition and awareness in Alzheimer disease. J. Geriatr. Psychiatry Neurol. 31, 27–33.

Belmeguenai, A., Hosy, E., Bengtsson, F., Pedroarena, C.M., Piochon, C., Teuling, E., He, Q., Ohtsuki, G., De Jeu, M.T., Elgersma, Y., De Zeeuw, C.I., Jorntell, H., Hansel, C., 2010. Intrinsic plasticity complements long-term potentiation in parallel fiber input gain control in cerebellar Purkinje cells. J. Neurosci. 30, 13630–13643.

Benussi, L., Binetti, G., Ghidoni, R., 2017. Loss of neuroprotective factors in neurodegenerative dementias: the end or the starting point? Front Neurosci. 11, 672.

Bliss, T.V., Collingridge, G.L., 1993. A synaptic model of memory: long-term potentiation in the hippocampus. Nature 361, 31–39.

Bond, W.S., Rex, T.S., 2014. Evidence that erythropoietin modulates Neuroinflammation through differential action on neurons, astrocytes, and microglia. Front Immunol. 5, 523.

Bonnas, C., Wustefeld, L., Winkler, D., Kronstein-Wiedemann, R., Dere, E., Specht, K., Boxberg, M., Tonn, T., Ehrenreich, H., Stadler, H., Sillaber, I., 2017. EV-3, an endogenous human erythropoietin isoform with distinct functional relevance. Sci. Rep. 7, 3684.

Brines, M., Cerami, A., 2005. Emerging biological roles for erythropoietin in the nervous system. Nat. Rev. Neurosci. 6, 484–494.

Brines, M.L., Ghezzi, P., Keenan, S., Agnello, D., de Lanerolle, N.C., Cerami, C., Itri, L.M., Cerami, A., 2000. Erythropoietin crosses the blood-brain barrier to protect against experimental brain injury. Proc. Natl. Acad. Sci. U S A. 97, 10526–10531.

Brines, M., Grasso, G., Fiordaliso, F., Sfacteria, A., Ghezzi, P., Fratelli, M., Latini, R., Xie, Q.W., Smart, J., Su-Rick, C.J., Pobre, E., Diaz, D., Gomez, D., Hand, C., Coleman, T., Cerami, A., 2004. Erythropoietin mediates tissue protection through an erythropoietin and common beta-subunit heteroreceptor. Proc. Natl. Acad. Sci. U S A. 101, 14907–14912.

Brines, M., Patel, N.S., Villa, P., Brines, C., Mennini, T., De Paola, M., Erbayraktar, Z., Erbayraktar, S., Sepodes, B., Thiemermann, C., Ghezzi, P., Yamin, M., Hand, C.C., Xie, Q.W., Coleman, T., Cerami, A., 2008. Nonerythropoietic, tissue-protective peptides derived from the tertiary structure of erythropoietin. Proc. Natl. Acad. Sci. U S A. 105, 10925–10930.

Buckner, R.L., 2004. Memory and executive function in aging and AD: multiple factors that cause decline and reserve factors that compensate. Neuron 44, 195–208.

Byts, N., Siren, A.L., 2009. Erythropoietin: a multimodal neuroprotective agent. Exp. Transl Stroke Med. 1, 4.

Cain, D.P., Hargreaves, E.L., Boon, F., Dennison, Z., 1993. An examination of the relations between hippocampal long-term potentiation, kindling, afterdischarge, and place learning in the water maze. Hippocampus 3, 153–163.

Celik, M., Gokmen, N., Erbayraktar, S., Akhisaroglu, M., Konakc, S., Ulukus, C., Genc, S., Genc, K., Sagiroglu, E., Cerami, A., Brines, M., 2002. Erythropoietin prevents motor neuron apoptosis and neurologic disability in experimental spinal cord ischemic injury. Proc. Natl. Acad. Sci. U S A. 99, 2258–2263.

Cerit, H., Veer, I.M., Dahan, A., Niesters, M., Harmer, C.J., Miskowiak, K.W., Rombouts, S.A.R.B., Van der Does, W., 2015. Testing the antidepressant properties of the peptide ARA290 in a human neuropsychological model of drug action. Eur. Neuropsychopharmacol. 25, 2289–2299.

Cheung Tung Shing, K.S., Broughton, S.E., Nero, T.L., Gillinder, K., Ilsley, M.D., Ramshaw, H., Lopez, A.F., Griffin, M.D.W., Parker, M.W., Perkins, A.C., Dhagat, U., 2018. EPO does not promote interaction between the erythropoietin and beta-common receptors. Sci. Rep. 8, 12457.

Chong, Z.Z., Li, F., Maiese, K., 2005. Erythropoietin requires NF-kappaB and its nuclear translocation to prevent early and late apoptotic neuronal injury during beta-amyloid toxicity. Curr. Neurovasc Res. 2, 387–399.

Chu, K., Jung, K.H., Lee, S.T., Kim, J.H., Kang, K.M., Kim, H.K., Lim, J.S., Park, H.K., Kim, M., Lee, S.K., Roh, J.K., 2008. Erythropoietin reduces epileptogenic processes following status epilepticus. Epilepsia 49, 1723–1732.

Chung, Y.H., Kim, S.I., Joo, K.M., Kim, Y.S., Lee, W.B., Yun, K.W., Cha, C.I., 2004. Age-related changes in erythropoietin immunoreactivity in the cerebral cortex and hippocampus of rats. Brain Res. 1018, 141–146.

Corbett, N.J., Gabbott, P.L., Klementiev, B., Davies, H.A., Colyer, F.M., Novikova, T., Stewart, M.G., 2013. Amyloid-beta induced CA1 pyramidal cell loss in young adult rats is alleviated by systemic treatment with FGL, a neural cell adhesion molecule-derived mimetic peptide. PLoS One 8, e71479.

D'Amelio, M., Rossini, P.M., 2012. Brain excitability and connectivity of neuronal assemblies in Alzheimer's disease: from animal models to human findings. Prog. Neurobiol. 99, 42–60.

Danielyan, L., Schafer, R., Schulz, A., Ladewig, T., Lourhmati, A., Buadze, M., Schmitt, A.L., Verleysdonk, S., Kabisch, D., Koeppen, K., Siegel, G., Proksch, B., Kluba, T., Eckert, A., Kohle, C., Schoneberg, T., Northoff, H., Schwab, M., Gleiter, C.H., 2009. Survival, neuron-like differentiation and functionality of mesenchymal stem cells in neurotoxic environment: the critical role of erythropoietin. Cell Death Differ 16, 1599–1614.

Delobette, S., Privat, A., Maurice, T., 1997. In vitro aggregation facilities beta-amyloid peptide-(25-35)-induced amnesia in the rat. Eur. J. Pharmacol. 319, 1–4.

Dhanushkodi, A., Akano, E.O., Roguski, E.E., Xue, Y., Rao, S.K., Matta, S.G., Rex, T.S., McDonald, M.P., 2013. A single intramuscular injection of rAAV-mediated mutant erythropoietin protects against MPTP-induced parkinsonism. Genes Brain Behav. 12, 224–233.

Dmytriyeva, O., Pankratova, S., Korshunova, I., Walmod, P.S., 2016. Epobis is a nonerythropoietic and neuroprotective agonist of the erythropoietin receptor with anti-inflammatory and memory enhancing effects. Mediators Inflamm. 2016, 1346390.
Ehrenreich, H., Degner, D., Meller, J., Brines, M., Behe, M., Hasselblatt, M., Woldt, H., Falkai, P., Knerlich, F., Jacob, S., von Ahsen, N., Maier, W., Bruck, W., Ruther, E., Cerami, A., Becker, W., Siren, A.L., 2004. Erythropoietin: a candidate compound for neuroprotection in schizophrenia. Mol. Psychiatry 9, 42–54.
Ehrenreich, H., Hinze-Selch, D., Stawicki, S., Aust, C., Knolle-Veentjer, S., Wilms, S., Heinz, G., Erdag, S., Jahn, H., Degner, D., Ritzen, M., Mohr, A., Wagner, M., Schneider, U., Bohn, M., Huber, M., Czernik, A., Pollmacher, T., Maier, W., Siren, A.L., Klosterkotter, J., Falkai, P., Ruther, E., Aldenhoff, J.B., Krampe, H., 2007. Improvement of cognitive functions in chronic schizophrenic patients by recombinant human erythropoietin. Mol. Psychiatry 12, 206–220.
El-Kordi, A., Radyushkin, K., Ehrenreich, H., 2009. Erythropoietin improves operant conditioning and stability of cognitive performance in mice. BMC Biol. 7, 37.
Enevoldsen, M.N., Kochoyan, A., Jurgenson, M., Jaako, K., Dmytriyeva, O., Walmod, P.S., Nielsen, J.D., Nielsen, J., Li, S., Korshunova, I., Klementiev, B., Novikova, T., Zharkovsky, A., Berezin, V., Bock, E., 2012. Neuroprotective and memory enhancing properties of a dual agonist of the FGF receptor and NCAM. Neurobiol. Dis. 48, 533–545.
Erbayraktar, S., Grasso, G., Sfacteria, A., Xie, Q.W., Coleman, T., Kreilgaard, M., Torup, L., Sager, T., Erbayraktar, Z., Gokmen, N., Yilmaz, O., Ghezzi, P., Villa, P., Fratelli, M., Casagrande, S., Leist, M., Helboe, L., Gerwein, J., Christensen, S., Geist, M.A., Pedersen, L.O., Cerami-Hand, C., Wuerth, J.P., Cerami, A., Brines, M., 2003. Asialoerythropoietin is a nonerythropoietic cytokine with broad neuroprotective activity in vivo. Proc. Natl. Acad. Sci. U S A. 100, 6741–6746.
Esmaeili Tazangi, P., Moosavi, S.M., Shabani, M., Haghani, M., 2015. Erythropoietin improves synaptic plasticity and memory deficits by decrease of the neurotransmitter release probability in the rat model of Alzheimer's disease. Pharmacol. Biochem. Behav. 130, 15–21.
Fares, R.P., Belmeguenai, A., Sanchez, P.E., Kouchi, H.Y., Bodennec, J., Morales, A., Georges, B., Bonnet, C., Bouvard, S., Sloviter, R.S., Bezin, L., 2013. Standardized environmental enrichment supports enhanced brain plasticity in healthy rats and prevents cognitive impairment in epileptic rats. PLoS One 8, e53888.
Fedotova, J., Soultanov, V., Nikitina, T., Roschin, V., Ordyan, N., Hritcu, L., 2016. Ropren(R) treatment reverses anxiety-like behavior and monoamines levels in gonadectomized rat model of Alzheimer's disease. Biomed. Pharmacother. 83, 1444–1455.
Gantner, D.C., Bailey, M., Presneill, J., French, C.J., Nichol, A., Little, L., Bellomo, R., 2017. Erythropoietin to reduce mortality in traumatic brain injury: a post-hoc dose-effect analysis. Ann. Surg. 267, 585–589.
Garrido Zinn, C., Clairis, N., Silva Cavalcante, L.E., Furini, C.R., de Carvalho, M., Izquierdo, J., 2016. I. Major neurotransmitter systems in dorsal hippocampus and basolateral amygdala control social recognition memory. Proc. Natl. Acad. Sci. U S A. 113, E4914–E4919.
Grimm, G., Stockenhuber, F., Schneeweiss, B., Madl, C., Zeitlhofer, J., Schneider, B., 1990. Improvement of brain function in hemodialysis patients treated with erythropoietin. Kidney Int. 38, 480–486.
Groticke, I., Hoffmann, K., Loscher, W., 2007. Behavioral alterations in the pilocarpine model of temporal lobe epilepsy in mice. Exp. Neurol. 207, 329–349.
Gundersen, H.J., Bagger, P., Bendtsen, T.F., Evans, S.M., Korbo, L., Marcussen, N., Moller, A., Nielsen, K., Nyengaard, J.R., Pakkenberg, B., Sørensen, F.B., Vesterby, A., West, M.J., 1988. The new stereological tools: disector, fractionator, nucleator and point sampled intercepts and their use in pathological research and diagnosis. APMIS 96, 857–881.
Jubinsky, P.T., Krijanovski, O.I., Nathan, D.G., Tavernier, J., Sieff, C.A., 1997. The beta chain of the interleukin-3 receptor functionally associates with the erythropoietin receptor. Blood 90, 1867–1873.
Jun, Y., JiangTao, X., YuanGui, H., YongBin, S., Jun, Z., XiaoJun, M., JianChun, X., Heng, X., XiaoXin, Z., XinXiang, X., 2009. Erythropoietin pre-treatment prevents cognitive impairments following status epilepticus in rats. Brain Res. 1282, 57–66.
Kamal, A., Al Shaibani, T., Ramakers, G., 2011. Erythropoietin decreases the excitatory neurotransmitter release probability and enhances synaptic plasticity in mice hippocampal slices. Brain Res. 1410, 33–37.
Kambova, L., 1998. Recombinant erythropoietin improves cognitive function in chronic haemodialysis patients. Nephrol. Dial Transplant. 13, 229–230.
Klementiev, B., Novikova, T., Novitskaya, V., Walmod, P.S., Dmytriyeva, O., Pakkenberg, B., Berezin, V., Bock, E., 2007. A neural cell adhesion molecule-derived peptide reduces neuropathological signs and cognitive impairment induced by Abeta25-35. Neuroscience 145, 209–224.
Klementiev, B., Li, S., Korshunova, I., Dmytriyeva, O., Pankratova, S., Walmod, P.S., Kjaer, L.K., Dahllof, M.S., Lundh, M., Christensen, D.P., Mandrup-Poulsen, T., Bock, E., Berezin, V., 2014. Anti-inflammatory properties of a novel peptide interleukin 1 receptor antagonist. J. Neuroinflammation 11, 27.
Kogan, J.H., Frankland, P.W., Silva, A.J., 2000. Long-term memory underlying hippocampus-dependent social recognition in mice. Hippocampus 10, 47–56.
Kristensen, P.L., Pedersen-Bjergaard, U., Kjaer, T.W., Olsen, N.V., Dela, F., Holst, J.J., Faber, J., Tarnow, L., Thorsteinsson, B., 2013. Influence of erythropoietin on cognitive performance during experimental hypoglycemia in patients with type 1 diabetes mellitus: a randomized cross-over trial. PLoS One 8, e59672.
Kumral, A., Uysal, N., Tugyan, K., Sonmez, A., Yilmaz, O., Gokmen, N., Kiray, M., Genc, S., Duman, N., Koroglu, T.F., Ozkan, H., Genc, K., 2004. Erythropoietin improves long-term spatial memory deficits and brain injury following neonatal hypoxia-ischemia in rats. Behav. Brain Res. 153, 77–86.
Lee, S.-T., Chu, K., Park, J.-E., Jung, K.-H., Jeon, D., Lim, J.-Y., Lee, S.K., Kim, M., Roh, J.-K., 2012. Erythropoietin improves memory function with reducing endothelial dysfunction and amyloid-beta burden in Alzheimer's disease models. J. Neurochem. 120, 115–124.
Leist, M., Ghezzi, P., Grasso, G., Bianchi, R., Villa, P., Fratelli, M., Savino, C., Bianchi, M., Nielsen, J., Gerwien, J., Kallunki, P., Larsen, A.K., Helboe, L., Christensen, S., Pedersen, L.O., Nielsen, M., Torup, L., Sager, T., Sfacteria, A., Erbayraktar, S., Erbayraktar, Z., Gokmen, N., Yilmaz, O., Cerami-Hand, C., Xie, Q.W., Coleman, T., Cerami, A., Brines, M., 2004. Derivatives of erythropoietin that are tissue protective but not erythropoietic. Science 305, 239–242.
Li, W., Maeda, Y., Yuan, R.R., Elkabes, S., Cook, S., Dowling, P., 2004. Beneficial effect of erythropoietin on experimental allergic encephalomyelitis. Ann. Neurol. 56, 767–777.
Li, X., Chen, Y., Shao, S., Tang, Q., Chen, W., Chen, Y., Xu, X., 2016a. Oxidative stress induces the decline of brain EPO expression in aging rats. Exp. Gerontol. 83, 89–93.
Li, Z.M., Xiao, Y.L., Zhu, J.X., Geng, F.Y., Guo, C.J., Chong, Z.L., Wang, L.X., 2016b. Recombinant human erythropoietin improves functional recovery in patients with severe traumatic brain injury: a randomized, double blind and controlled clinical trial. Clin. Neurol. Neurosurg. 150, 80–83.
Liu, Q., Shi, J., Lin, R., Wen, T., 2017. Dopamine and dopamine receptor D1 associated with decreased social interaction. Behav. Brain Res. 324, 51–57.
Lourhmati, A., Buniatian, G.H., Paul, C., Verleysdonk, S., Buecheler, R., Buadze, M., Proksch, B., Schwab, M., Gleiter, C.H., Danielyan, L., 2013. Age-dependent astroglial vulnerability to hypoxia and glutamate: the role for erythropoietin. PLoS One 8, e77182.
Lu, D., Mahmood, A., Qu, C., Goussev, A., Schallert, T., Chopp, M., 2005. Erythropoietin enhances neurogenesis and restores spatial memory in rats after traumatic brain injury. J. Neurotrauma 22, 1011–1017.
Ma, R., Xiong, N., Huang, C., Tang, Q., Hu, B., Xiang, J., Li, G., 2009. Erythropoietin protects PC12 cells from beta-amyloid(25-35)-induced apoptosis via PI3K/Akt signaling pathway. Neuropharmacology 56, 1027–1034.
Maiese, K., Chong, Z.Z., Shang, Y.C., Wang, S., 2012. Erythropoietin: new directions for the nervous system. Int. J. Mol. Sci. 13, 11102–11129.
Maurice, T., Mustafa, M.H., Desrumaux, C., Keller, E., Naert, G., de la, C.G.-B.M., Rodriguez Cruz, Y., Garcia Rodriguez, J.C., 2013. Intranasal formulation of erythropoietin (EPO) showed potent protective activity against amyloid toxicity in the Abeta(2)(5)(-)(3)(5) non-transgenic mouse model of Alzheimer's disease. J. Psychopharmacol. 27, 1044–1057.
McCagh, J., Fisk, J.E., Baker, G.A., 2009. Epilepsy, psychosocial and cognitive functioning. Epilepsy Res. 86, 1–14.
Meldolesi, J., 2011. Neurite outgrowth: this process, first discovered by Santiago Ramon y Cajal, is sustained by the exocytosis of two distinct types of vesicles. Brain Res. Rev. 66, 246–255.
Metcalfe, S.M., Bickerton, S., Fahmy, T., 2017. Neurodegenerative disease: a perspective on cell-based therapy in the new era of cell-free Nano-therapy. Curr. Pharm. Des. 23, 776–783.
Miskowiak, K., O'Sullivan, U., Harmer, C.J., 2007. Erythropoietin enhances hippocampal response during memory retrieval in humans. J. Neurosci. 27, 2788–2792.
Miskowiak, K., Inkster, B., O'Sullivan, U., Selvaraj, S., Goodwin, G.M., Harmer, C.J., 2008a. Differential effects of erythropoietin on neural and cognitive measures of executive function 3 and 7 days post-administration. Exp. Brain Res. 184, 313–321.
Miskowiak, K., Inkster, B., Selvaraj, S., Wise, R., Goodwin, G.M., Harmer, C.J., 2008b. Erythropoietin improves mood and modulates the cognitive and neural processing of emotion 3 days post administration. Neuropsychopharmacology 33, 611–618.
Miskowiak, K.W., Vinberg, M., Harmer, C.J., Ehrenreich, H., Kessing, L.V., 2012. Erythropoietin: a candidate treatment for mood symptoms and memory dysfunction in depression. Psychopharmacology 219, 687–698.
Miskowiak, K.W., Ehrenreich, H., Christensen, E.M., Kessing, L.V., Vinberg, M., 2014. Recombinant human erythropoietin to target cognitive dysfunction in bipolar disorder: a double-blind, randomized, placebo-controlled phase 2 trial. J. Clin. Psychiatry 75, 1347–1355.
Mogensen, J., Jensen, C., Kingod, S.C., Hansen, A., Larsen, J.A., Mala, H., 2008. Erythropoietin improves spatial delayed alternation in a T-maze in fimbria-fornix transected rats. Behav. Brain Res. 186, 215–221.
Morishita, E., Masuda, S., Nagao, M., Yasuda, Y., Sasaki, R., 1997. Erythropoietin receptor is expressed in rat hippocampal and cerebral cortical neurons, and erythropoietin prevents in vitro glutamate-induced neuronal death. Neuroscience 76, 105–116.
Muller, C.J., Bankstahl, M., Groticke, I., Loscher, W., 2009. Pilocarpine vs. lithium-pilocarpine for induction of status epilepticus in mice: development of spontaneous seizures, behavioral alterations and neuronal damage. Eur. J. Pharmacol. 619, 15–24.
Nadam, J., Navarro, F., Sanchez, P., Moulin, C., Georges, B., Laglaine, A., Pequignot, J.M., Morales, A., Ryvlin, P., Bezin, L., 2007. Neuroprotective effects of erythropoietin in the rat hippocampus after pilocarpine-induced status epilepticus. Neurobiol. Dis. 25, 412–426.
Ning, B., Zhang, A., Song, H., Gong, W., Ding, Y., Guo, S., Zhao, Y., Jiang, J., Jia, T., 2011. Recombinant human erythropoietin prevents motor neuron apoptosis in a rat model of cervical sub-acute spinal cord compression. Neurosci. Lett. 490, 57–62.
Ostrowski, D., Heinrich, R., 2018. Alternative erythropoietin receptors in the nervous system. J. Clin. Med. 7.

Ott, C., Martens, H., Hassouna, I., Oliveira, B., Erck, C., Zafeiriou, M.P., Peteri, U.K., Hesse, D., Gerhart, S., Altas, B., Kolbow, T., Stadler, H., Kawabe, H., Zimmermann, W.H., Nave, K.A., Schulz-Schaeffer, W., Jahn, O., Ehrenreich, H., 2015. Widespread expression of erythropoietin receptor in brain and its induction by injury. Mol. Med. 21, 803–815.

Pankratova, S., Kiryushko, D., Sonn, K., Soroka, V., Kohler, L.B., Rathje, M., Gu, B., Gotfryd, K., Clausen, O., Zharkovsky, A., Bock, E., Berezin, V., 2010. Neuroprotective properties of a novel, non-haematopoietic agonist of the erythropoietin receptor. Brain 133, 2281–2294.

Pankratova, S., Gu, B., Kiryushko, D., Korshunova, I., Kohler, L.B., Rathje, M., Bock, E., Berezin, V., 2012. A new agonist of the erythropoietin receptor, Epobis, induces neurite outgrowth and promotes neuronal survival. J. Neurochem. 121, 915–923.

Pickett, J.L., Theberge, D.C., Brown, W.S., Schweitzer, S.U., Nissenson, A.R., 1999. Normalizing hematocrit in dialysis patients improves brain function. Am. J. Kidney Dis. 33, 1122–1130.

Robertson, C.S., Garcia, R., Gaddam, S.S., Grill, R.J., Cerami Hand, C., Tian, T.S., Hannay, H.J., 2013. Treatment of mild traumatic brain injury with an erythropoietin-mimetic peptide. J. Neurotrauma 30, 765–774.

Rodriguez Cruz, Y., Strehaiano, M., Rodriguez Obaya, T., Garcia Rodriguez, J.C., Maurice, T., 2017. An intranasal formulation of erythropoietin (Neuro-EPO) prevents memory deficits and amyloid toxicity in the APPSwe transgenic mouse model of Alzheimer's disease. J. Alzheimers Dis. 55, 231–248.

Rudenko, O., Tkach, V., Berezin, V., Bock, E., 2010. Effects of FGF receptor peptide agonists on animal behavior under normal and pathological conditions. Neurosci. Res. 68, 35–43.

Sakanaka, M., Wen, T.C., Matsuda, S., Masuda, S., Morishita, E., Nagao, M., Sasaki, R., 1998. In vivo evidence that erythropoietin protects neurons from ischemic damage. Proc. Natl. Acad. Sci. U S A. 95, 4635–4640.

Sanchez, P.E., Fares, R.P., Risso, J.J., Bonnet, C., Bouvard, S., Le-Cavorsin, M., Georges, B., Moulin, C., Belmeguenai, A., Bodennec, J., Morales, A., Pequignot, J.M., Baulieu, E.E., Levine, R.A., Bezin, L., 2009. Optimal neuroprotection by erythropoietin requires elevated expression of its receptor in neurons. Proc. Natl. Acad. Sci. U S A. 106, 9848–9853.

Sargin, D., Friedrichs, H., El-Kordi, A., Ehrenreich, H., 2010. Erythropoietin as neuroprotective and neuroregenerative treatment strategy: comprehensive overview of 12 years of preclinical and clinical research. Best Pract. Res. Clin. Anaesthesiol 24, 573–594.

Sargin, D., El-Kordi, A., Agarwal, A., Muller, M., Wojcik, S.M., Hassouna, I., Sperling, S., Nave, K.A., Ehrenreich, H., 2011. Expression of constitutively active erythropoietin receptor in pyramidal neurons of cortex and hippocampus boosts higher cognitive functions in mice. BMC Biol. 9, 27.

Saunders, N.R., Habgood, M.D., Dziegielewska, K.M., 1999. Barrier mechanisms in the brain, I. Adult brain. Clin. Exp. Pharmacol. Physiol. 26, 11–19.

Secher, T., Novitskaia, V., Berezin, V., Bock, E., Glenthoj, B., Klementiev, B., 2006. A neural cell adhesion molecule-derived fibroblast growth factor receptor agonist, the FGL-peptide, promotes early postnatal sensorimotor development and enhances social memory retention. Neuroscience 141, 1289–1299.

Shang, Y.C., Chong, Z.Z., Wang, S., Maiese, K., 2012. Prevention of beta-amyloid degeneration of microglia by erythropoietin depends on Wnt1, the PI 3-K/mTOR pathway, Bad, and Bcl-xL. Aging (Albany NY) 4, 187–201.

Simpson, J.E., Ince, P.G., Lace, G., Forster, G., Shaw, P.J., Matthews, F., Savva, G., Brayne, C., Wharton, S.B., 2010. Astrocyte phenotype in relation to Alzheimer-type pathology in the ageing brain. Neurobiol. Aging 31, 578–590.

Siren, A.L., Fratelli, M., Brines, M., Goemans, C., Casagrande, S., Lewczuk, P., Keenan, S., Gleiter, C., Pasquali, C., Capobianco, A., Mennini, T., Heumann, R., Cerami, A., Ehrenreich, H., Ghezzi, P., 2001. Erythropoietin prevents neuronal apoptosis after cerebral ischemia and metabolic stress. Proc. Natl. Acad. Sci. U S A. 98, 4044–4049.

Siren, A.L., Fasshauer, T., Bartels, C., Ehrenreich, H., 2009. Therapeutic potential of erythropoietin and its structural or functional variants in the nervous system. Neurotherapeutics 6, 108–127.

Sozmen, S.C., Kurul, S.H., Yis, U., Tugyan, K., Baykara, B., Yilmaz, O., 2012. Neuroprotective effects of recombinant human erythropoietin in the developing brain of rat after lithium-pilocarpine induced status epilepticus. Brain Dev. 34, 189–195.

Statler, P.A., McPherson, R.J., Bauer, L.A., Kellert, B.A., Juul, S.E., 2007. Pharmacokinetics of high-dose recombinant erythropoietin in plasma and brain of neonatal rats. Pediatr. Res. 61, 671–675.

Sun, Z.K., Yang, H.Q., Pan, J., Zhen, H., Wang, Z.Q., Chen, S.D., Ding, J.Q., 2008. Protective effects of erythropoietin on tau phosphorylation induced by beta-amyloid. J. Neurosci. Res. 86, 3018–3027.

Syed, R.S., Reid, S.W., Li, C., Cheetham, J.C., Aoki, K.H., Liu, B., Zhan, H., Osslund, T.D., Chirino, A.J., Zhang, J., Finer-Moore, J., Elliott, S., Sitney, K., Katz, B.A., Matthews, D.J., Wendoloski, J.J., Egrie, J., Stroud, R.M., 1998. Efficiency of signalling through cytokine receptors depends critically on receptor orientation. Nature 395, 511–516.

Upadhyay, R.K., 2014. Drug delivery systems, CNS protection, and the blood brain barrier. Biomed. Res. Int. 2014, 869269.

Uzum, G., Sarper Diler, A., Bahcekapili, N., Ziya Ziylan, Y., 2006. Erythropoietin prevents the increase in blood-brain barrier permeability during pentylentetrazol induced seizures. Life Sci. 78, 2571–2576.

Walsh, D.M., Selkoe, D.J., 2004. Deciphering the molecular basis of memory failure in Alzheimer's disease. Neuron 44, 181–193.

Wang, B., Kang, M., Marchese, M., Rodriguez, E., Lu, W., Li, X., Maeda, Y., Dowling, P., 2016. Beneficial effect of erythropoietin short peptide on acute traumatic brain injury. Neurotherapeutics 13, 418–427.

Xenocostas, A., Cheung, W.K., Farrell, F., Zakszewski, C., Kelley, M., Lutynski, A., Crump, M., Lipton, J.H., Kiss, T.L., Lau, C.Y., Messner, H.A., 2005. The pharmacokinetics of erythropoietin in the cerebrospinal fluid after intravenous administration of recombinant human erythropoietin. Eur. J. Clin. Pharmacol. 61, 189–195.

Xiong, Y., Mahmood, A., Meng, Y., Zhang, Y., Qu, C., Schallert, T., Chopp, M., 2009. Delayed administration of erythropoietin reducing hippocampal cell loss, enhancing angiogenesis and neurogenesis, and improving functional outcome following traumatic brain injury in rats: comparison of treatment with single and triple dose. J. Neurosurg. 113, 598–608.

Yu, X., Shacka, J.J., Eells, J.B., Suarez-Quian, C., Przygodzki, R.M., Beleslin-Cokic, B., Lin, C.S., Nikodem, V.M., Hempstead, B., Flanders, K.C., Costantini, F., Noguchi, C.T., 2002. Erythropoietin receptor signalling is required for normal brain development. Development 129, 505–516.

Zellinger, C., Seeger, N., Hadamitzky, M., Fischborn, S., Russmann, V., Wendt, H., Pankratova, S., Bock, E., Berezin, V., Potschka, H., 2011. Impact of the erythropoietin-derived peptide mimetic Epotris on the histopathological consequences of status epilepticus. Epilepsy Res. 96, 241–249.

Zhang, S.J., Wang, R.L., Zhao, H.P., Tao, Z., Li, J.C., Ju, F., Han, Z.P., Ma, Q.F., Liu, P., Ma, S.B., Cao, G.D., Luo, Y.M., 2019. MEPO promotes neurogenesis and angiogenesis but suppresses gliogenesis in mice with acute ischemic stroke. Eur. J. Pharmacol. 849, 1–10.

Zussy, C., Brureau, A., Delair, B., Marchal, S., Keller, E., Ixart, G., Naert, G., Meunier, J., Chevallier, N., Maurice, T., Givalois, L., 2011. Time-course and regional analyses of the physiopathological changes induced after cerebral injection of an amyloid beta fragment in rats. Am. J. Pathol. 179, 315–334.